ELSEVIER

Coordination Chemistry Reviews
215 (2001) 301–345

COORDINATION CHEMISTRY REVIEWS

www.elsevier.com/locate/ccr

Nitride chemistry of the s-block elements

Duncan H. Gregory

School of Chemistry, University of Nottingham, University Park, Nottingham NG7 2RD, UK

Received 6 October 2000; accepted 20 November 2000

Dedicated to Dr Richard J. Pulham on the occasion of his retirement.

Contents

Abstract . . . 301
1. Introduction and scope of this review . . . 302
2. Nitrides of the alkali metals . . . 303
   2.1 The lithium–nitrogen system . . . 303
      2.1.1 α-Li_3N . . . 303
      2.1.2 β- and γ-Li_3N . . . 310
   2.2 Nitrides of the heavier alkali metals . . . 312
3. Alkaline earth metal nitrides . . . 313
   3.1 Structural trends . . . 313
   3.2 'Ionic' nitrides . . . 314
      3.2.1 Beryllium nitride . . . 314
      3.2.2 Magnesium nitride . . . 315
      3.2.3 Calcium nitrides . . . 317
      3.2.4 Other compositions . . . 322
   3.3 Binary and higher subnitrides . . . 323
4. Ternary nitrides of the s-block metals . . . 333
   4.1 Group 1/group 2 compounds . . . 333
   4.2 Group 2 compounds . . . 337
5. Concluding remarks . . . 340
Acknowledgements . . . 340
References . . . 340

Abstract

The highly electropositive s-block elements combine with nitrogen in the solid state to form some of the most ionic nitride compounds known. Also, however, these elements can

E-mail address: duncan.gregory@nottingham.ac.uk (D.H. Gregory).

PII: S0010-8545(01)00320-4

combine in binary and higher systems to form compounds with partially covalent character, predominantly metallic bonds or low dimensional structural hybrids of metallic and ionic components. The crystal and coordination chemistry of both binary and ternary s-block nitrides is unusual and provides the basis for unexpected and exploitable physical properties and a range of exotic reaction chemistry.

Keywords: Nitride chemistry; s-Block elements; Nitrogen; Structure; Properties

1. Introduction and scope of this review

Progress in nitride chemistry has been significant within the last several years [1,2]. The extent of this progress is manifested not only in the improved classification of nitride crystal chemistry and development of new synthetic techniques, but also in the emergence of genuine nitride materials. Numerous binary compounds from most regions of the periodic table (many of which were first synthesised over 50 years ago) are now well characterised. Increasingly, this is true of ternary and higher nitrides also. It is a testament to the skill and vision of the original researchers in this area and latterly to improvements in synthetic methods and analytical techniques, that nitride chemistry has evolved as it has. Significant challenges to the solid state chemist remain, however. Not least are the thermodynamic barriers that need to be overcome to synthesise nitrides at the outset. The role of thermodynamics in designing a preparative methodology perhaps remains the single largest constraint checking growth in the area and accounts for the relatively low abundance of these solids. It is also, however, thermodynamics that shapes valence and bonding in nitrides, with truly ionic compounds incorporating N^{3-} found only with combinations of nitrogen with the most electropositive of elements. The use of the inductive effect demonstrated by these electropositive metals, as described by Etourneau et al. [3], has allowed the stabilisation of other metal–nitrogen bonds in ternary and higher compounds that would be otherwise unstable. What perhaps is less obvious, however, is that the binary and higher compounds of the electropositive s-block elements with nitrogen are not universally the classically ionic compounds we might expect. In fact, the nitrides of the s-block elements, like many of their counterparts from elsewhere in the periodic table, demonstrate a rich mix of valence and bonding behaviour leading to highly varied structural and reaction chemistry and a surprisingly wide array of unusual physical properties.

Previous reviews in the literature have covered the many different aspects of nitride chemistry. The emphasis has chiefly tended to fall on compounds of the transition elements [1,2] but increasingly nitrides of the p-block elements have become more important and prevalent. This is especially true of the work performed principally by Schnick et al. in nitridosilicate and nitridophosphate chemistry [4–6], by DiSalvo et al. in nitridogermanate chemistry [7–9] and is also represented, for example, by the continued development of group 13 nitrides as refractory ceramics, coatings, semiconductors and optical materials. The focus of

this article, however, will be the nitrides formed by the elements of groups 1 and 2, a subject perhaps neglected in reviews of the area. In fact, only a small number of recent review articles exist that specifically cover some of the nitrides of the alkali and alkaline earth metals described herein. The reader is directed to papers by Simon [10] and Röhr [11], for example, for detailed historical accounts of the former author's subnitride research (which is also set within the wider context of suboxides). Also, it should be noted that further general structural information regarding group 1 and 2 nitrides can be found within Brese and O'Keeffe's definitive 1992 review of nitride crystal chemistry [12].

2. Nitrides of the alkali metals

Alkali metal nitride chemistry is dominated by lithium nitride, Li_3N, a compound that has long fascinated solid state chemists since early reports of its synthesis and characterisation [13–15]. The existence of binary nitrides of the heavier alkali metals is debatable and at best, these compounds can be described as unstable.

2.1. The lithium–nitrogen system

Initial developments in the characterisation of lithium nitride (α-Li_3N) took place in the 1930s with the successful structural determination of Li_3N from single crystal diffraction data by Zintl and Brauer [15]. Significant advances were made several decades later as then state of the art techniques were used for the first time to elucidate links between this unique structure and the observed physical properties first predicted approximately 30 years beforehand in 1948 [16]. The salient features of this intense period of research are summarised elegantly by von Alpen [17] and Rabenau [18]. Arguably, lithium nitride is the most-studied, best-elucidated nitride to-date. More recently evidence for other phases in the Li–N system has been presented.

2.1.1. α-Li_3N

Lithium nitride can be readily synthesised in a number of ways. Arguably the easiest of these is via the reaction of solid lithium with nitrogen gas at elevated temperatures. In fact, this reaction begins to occur under ambient conditions. The disadvantage of such a technique, however, lies in the nature of the product-often poorly crystalline and frequently contaminated by lithium oxide, hydroxide or carbonate unless stringent anaerobic, anhydrous conditions are observed. Highly (poly)crystalline bulk product is obtained via liquid metals approaches by the reaction of nitrogen with liquid lithium or alternatively with solid lithium dissolved in liquid sodium [19–21]. The Li–Li_3N phase diagram is remarkably simple, showing a single eutectic at a composition close to pure Li [22]. Beyond this a smooth liquidus exists over the entire composition range from the melting point of lithium (reported in the original phase study as 185°C as opposed to 180.5°C) to that of Li_3N (815°C) [23]. Methods focusing on the Li–Li_3N system can be thus

adapted to promote growth of sizeable single crystals (approximately 3 cm length, 1 cm thickness) by the Czochralski technique [24]. Crystals are so grown from an Li melt contained in a tungsten crucible within a steel autoclave operating at a maximum N_2 pressure of 700 Torr. Whereas finely divided polycrystalline powders of Li_3N are extremely air-sensitive (forming LiOH and ammonia), these large, ruby red crystals are stable in a moist atmosphere for several days. This is due, somewhat perversely, to the formation of a surface film of predominantly LiOH (ΔG_f $Li_3N = -128.6$ kJ mol^{-1} [25] cf. ΔG_f LiOH $= -497$ kJ mol^{-1} [26][DHG1]).

The crystal structure of α-Li_3N as originally solved by Zintl and Brauer [15] and as re-determined by Rabenau and Schultz [27] is shown in Fig. 1. The structure is unique to lithium nitride and consists of graphite-like hexagonal layers (similar to those in BN) of planar lithium hexagons centred by nitrogen. Each NLi_6 hexagon in the [Li_2N] layer is capped above and below the *ab* plane by a further lithium ion, connecting the layers in the third dimension (along c). Hence each nitrogen atom is coordinated by a total of eight lithium atoms in hexagonal bipyramidal geometry. Lithium atoms within [Li_2N] planes are in a trigonal planar coordination geometry with N, whereas those between planes are linearly coordinated to nitrogen.

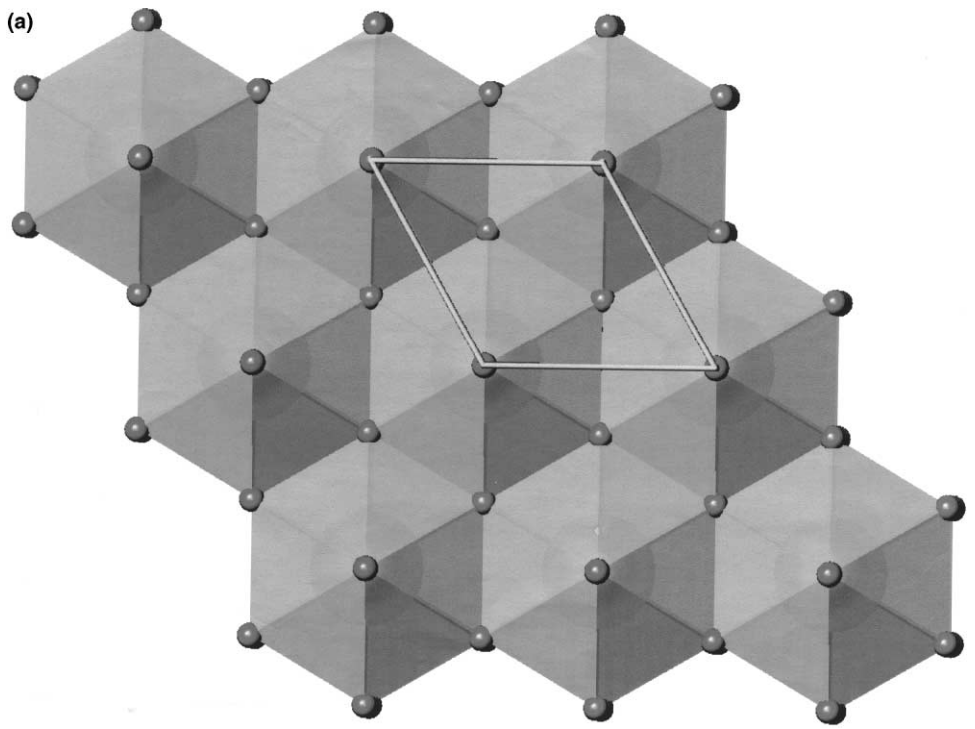

Fig. 1. Polyhedral representation of the structure of α-Li_3N (a) as a projection on the [001] plane showing [Li_2N] layers of edge-sharing NLi_8 hexagonal bipyramids; (b) showing vertex linking of NLi_8 hexagonal bipyramids along the *c*-axis. Small spheres represent Li, large spheres within polyhedra represent N.

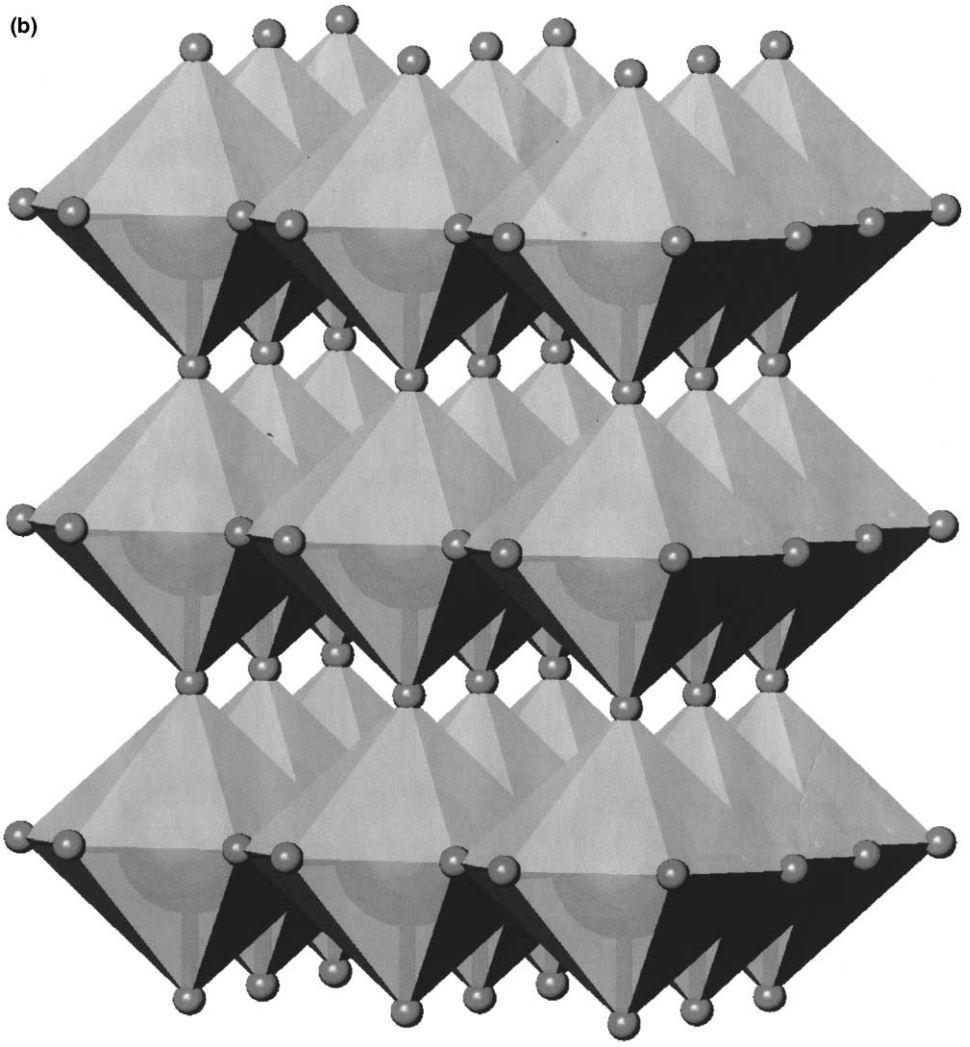

Fig. 1. (*Continued*)

Many of the physical properties of Li_3N are apparently anomalous and this has prompted continued and detailed study of structure and bonding within the compound using a large variety of techniques. Lithium nitride is bright red (in fact, colours from ruby red through to dark purple can be observed) which is unexpected for an ostensibly ionic compound of this type. Also, however, early measurements showed that polycrystalline Li_3N has an exceptionally high Li-ion conductivity (approximately $10^{-4}\ \Omega^{-1}\ cm^{-1}$) [28] with potential application as a solid electrolyte in lithium ion batteries. The principal acknowledged challenge to be overcome in the use of the nitridolithiate as such a material is its low thermody-

namic decompostion potential (0.44 V at room temperature). The conduction mechanism is not obvious from the originally described crystal structure. A combination of diffraction, Compton scattering, NMR, infrared and Raman spectroscopy, lattice dynamics and theoretical techniques have revealed the likely true nature of the crystal structure and bonding in Li_3N.

Variable temperature single crystal X-ray diffraction studies illustrated in the first instance that Li_3N was composed of Li^+ anions and N^{3-} cations on the basis of calculating scattering curves from Watson-sphere potentials for the ions versus the atoms in Li_3N [29]. Here, importantly, N^{3-} is stabilised (relative to the free ion) by the presence of surrounding Li^+ cations. Infrared and Raman spectroscopic studies performed at this time also elucidated the lattice dynamics of the compound and lent significant weight to the existence of the highly polarisable N^{3-} anion in lithium nitride [30]. Further evidence for the ionic bonding model exists from room temperature coherent inelastic neutron scattering experiments [31] and Compton scattering investigations [32–34]. The former work showed that the experimental phonon dispersion curves were well modelled by shells incorporating long-range Coulomb interactions between N^{3-} and Li^+, short range interactions between neighbouring ions and an anisotropic electronic polarisability of the N^{3-} anion. The Compton scattering studies supported these findings and emphasised the significance of the N^{3-} anisotropy in generating a more sophisticated and accurate model than one based purely on a Watson sphere approach. First principles pseudopotential calculations performed in 1981 confirmed the ionic picture of bonding in lithium nitride describing nitride anions with an associated charge of -2.8 [35]. The method also delineates a band structure for Li_3N in semi-quantitative agreement with optical measurements [36]. Both theoretical and experimental techniques define an indirect band gap. Optical measurements were performed with incident light perpendicular and parallel to the c-direction. Calculated values are approximately 1 eV smaller than those observed experimentally ($E//c = 2.15$ eV at 4.2 K, $E \perp c \approx 2.1$ eV at 4.2 K via optical absorption). The indirect band gap exists between effectively a filled N 2p valence band and a broad, vacant Li 2s band. Later Hartree–Fock calculations also reinforced experimental results [37,38] and the nitride anion in α-Li_3N was revealed to be approximately 200 times as polarisable as the lithium cation [39].

Subsequently, diffraction techniques were used to demonstrate that even at low temperature (153 K) the lithium position within the $[Li_2N]$ planes (Li(2)) is underoccupied by 1–2%. This occupation remains constant until approximately 570 K, but by 678 K the site occupancy drops to 96% [40]. By modelling anharmonic effects, the Li(2) site occupancy at 888 K was observed to drop to 93(1)% [41]. The proposed origin of the defects in Li_3N is the disordered doping of small amounts of imide, $(NH)^{2-}$ for N^{3-} on the nitrogen sites in the $[Li_2N]$ plane. This is evident in seemingly pure Li_3N from infrared transmission spectroscopy [42] and in both 'pure' and intentionally H-doped Li_3N via infrared spectroscopy [43,44]. The latter studies especially indicate a correlation of increasing ionic conductivity with increasing H content (and therefore, $(NH)^{2-}$ concentration). This premise tends to support not only the requirements of charge balance but also the non-observation

of electronic conductivity experimentally. Single crystal neutron diffraction of Li_3N doped with <1 at.% D, suggests a composition $Li_{2.95}ND_{0.02}$ with D partially occupying (0.19(4)%) the 6*j* (*x*,0,0) site to give disordered ND^{2-} anions within the Li_3N structure and retention of the parent space group *P6/mmm* (Fig. 2) [45].

Conductivity measurements performed on single crystals of Li_3N indicate a high degree of anisotropy with values perpendicular to the *c*-axis (i.e. parallel to the $[Li_2N]$ layers and the *ab* plane) two orders of magnitude higher than those parallel to *c* at 300 K (Table 1) [46]. These observations have been rationalised and a diffusion mechanism proposed by diffraction, solid state nuclear-magnetic resonance (NMR) and calculation. Study of the anisotropic temperature profiles and residual electron density maps from single crystal X-ray diffraction measurements favours a direct hopping mechanism of Li(2) ions sitting in shallow potential wells in the $[Li_2N]$ planes. An alternative mechanism involving hopping through the Li(1) layer requires a considerably higher activation energy in agreement with the observed conductivity data [40,41]. Initial ^{7}Li-NMR experiments performed on powders seemed to favour a covalent description of Li_3N based on the perceived size of the field gradients at the Li nuclei [47,48] but subsequent NMR examinations

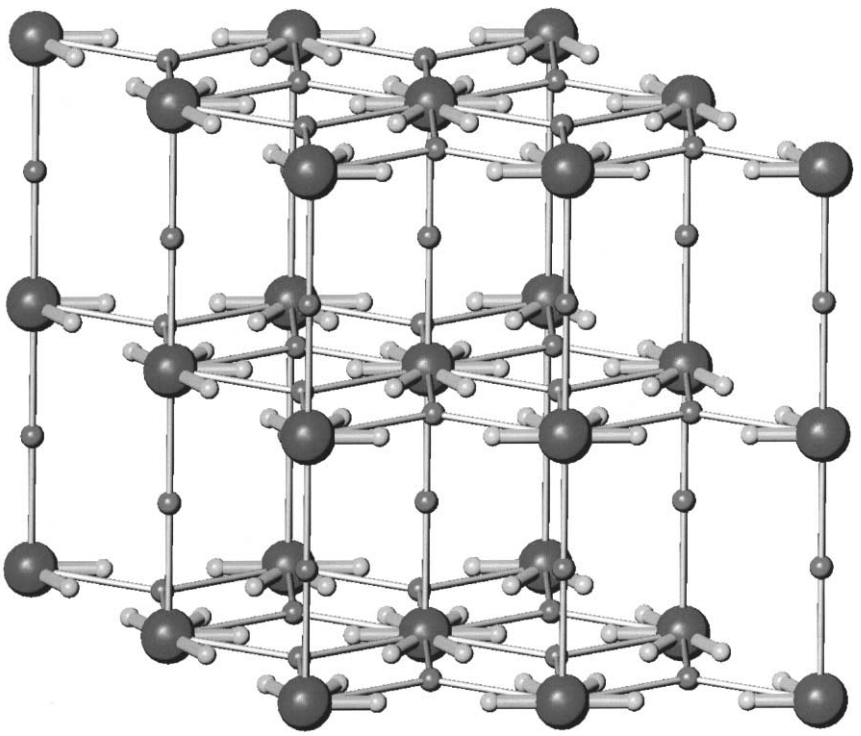

Fig. 2. Structure of $Li_{3-x-y}ND_y$ ($y \approx 0.02$). The deuterium doped nitride retains the space group of Li_3N (*P6/mmm*) with D (smallest light spheres) disordered in the 6*j* position (0.19(4)% occupied) [45]. Lithium atoms are depicted as small spheres, N as large spheres.

Table 1
Selected anisotropic physical properties of α-Li_3N

Direction	⊥ *c*-Axis	// *c*-Axis	⊥ *c*/// *c*	References
Dielectric constant, γ_0 (300 K)	10.5	6	1.75	[30]
Conductivity, σ (300 K) Ω^{-1} cm^{-1}	1.2×10^{-3}	1×10^{-5}	120	[46]
Conductivity, σ (400 K) Ω^{-1} cm^{-1}	8×10^{-3}	6×10^{-4}	13.3	[46]
Conductivity, σ (500 K) Ω^{-1} cm^{-1}	4×10^{-2}	8×10^{-3}	5	[46]
Diffusion coefficient, *D* (800 K) m^2 s^{-1} — NMR	7.8×10^{-10}	4.2×10^{-10}	1.9	[54]
Diffusion coefficient, *D* (800 K) m^2 s^{-1} — theory	3.4×10^{-8}	1.3×10^{-8}	2.6	[60]
Activation enthalpy, *H* (eV) — σ	0.29	0.49	0.6	[46]
Activation enthalpy, *H* (eV) — X-ray diffraction	0.29 (4)	–	–	[41]
Activation enthalpy, *H* (eV) — NMR	0.41	0.68	0.6	[54]
Band gap (4.2 K) (eV) — optical absorption	2.15	≈2.1	1	[36]

of single crystals proved the ionic model of Li_3N more likely to be correct [49,50]. Here the two coupling constants observed from the quadrupolar ^7Li splitting in the spectrum could be attributed to the Li(1) and Li(2) sites (coupling constants of 582 ± 2 and 285 ± 2 kHz, respectively) [50]. Calculation of electric field gradients and charge density at the three crystallographic sites in α-Li_3N consequently agreed well with experimental results [51,52]. The above and later NMR studies (including application of β-radiation detected NMR to ^8Li nuclei) also confirmed that the principle mechanism for conduction was the diffusion of Li^+ ions in the $[Li_2N]$ planes but importantly provided detailed information regarding the less favourable diffusion of Li^+ ions across the Li(1) layers [53–55]. The NMR evidence confirms conduction within $[Li_2N]$ planes ($\perp c$) only involves the Li(2) position and is dependent on H (NH^{2-}) concentration whereas conduction parallel to the *c*-axis ($//c$) involves both Li(1) and Li(2) sites and shows no such dependence [53]. The NMR studies reinforce observations that the activation enthalpy perpendicular to *c* (H $\perp c$) is lower than that parallel to *c*, (H $//c$), although the contrast between these two processes is not as great as indicated by conductivity measurements (also described in Table 1) [54]. Molecular dynamics simulations of Li_3N elucidate further the diffusion mechanisms at low temperature and above. These indicate that at low temperatures (150, 300 K) the Li^+ transport is confined principally to the $[Li_2N]$ planes whereas at elevated temperatures (400 K and above), conduction both parallel and perpendicular to *c* operates through interstitial sites above and below the N-centred hexagonal layers [56–59]. Recent ab initio molecular dynamics calculations have provided a good illustration of the anisotropy in the diffusion process in α-Li_3N and provided activation energies and diffusion coefficients in reasonable agreement with experiment [60].

The reaction chemistry of α-Li_3N is extensive and will be surveyed only briefly here, highlighting some of the more interesting compounds currently known. A more detailed overview of resulting compounds mentioned below and others can be

found elsewhere [1,2,12,61]. Nitride compounds formed between lithium and alkaline earth metals are discussed in Section 4.

Lithium nitride reacts with first row transition metals (M) at moderate to high temperatures (typically approximately 600–900°C) to form principally compounds within one of two structure groupings. Compounds of the earlier elements (M = Ti–Fe) form anti-fluorite superstructures of general formulation $[(Li,M)_2N]_n$ in which the transition metal is usually in its highest stable oxidation state. Most of the structures exhibit Li/M ordering depending on stoichiometry (and hence M oxidation state). Examples thus include, Li_5TiN_3, Li_7VN_4, 'Li_9CrN_5', Li_7MnN_4, Li_3FeN_2 [61]. The likely identity of the chromium compound was subsequently suspected to be a defect anti-fluorite variant of stoichiometry, $Li_{14}Cr_2N_8O$ or $Li_{14}Cr_2N_8(NH)$. $Li_{15}Cr_2N_9$ is also known [62]. Later first row transition metals (M = Fe–Cu) form substituted variants of the α-Li_3N structure itself, $Li_{3-x}M_xN$ ($0 \leq x \leq 0.4$), with M substituting for lithium at the Li(1) site between $[Li_2N]$ planes [61]. Subsequent study has revealed creation of additional lithium vacancies under certain synthetic conditions. These compounds have compositions $Li_{3-x-y}M_x\square_yN$ (□ = vacancy) with vacancies concomitant with transition metal substitution [63–67]. Vacancies can be ordered or disordered in the α-Li_3N derived structure. Iron is unique to date in that it forms ternary nitrides with both anti-fluorite related (Li_3FeN_2) and Li_3N-type (Li_4FeN_2) structures [63,68]. LiZnN reportedly forms with an ordered anti-fluorite structure [69,70]. Manganese also forms $(Li,Mn)_2N$ with the anti-rutile structure [71]. Heavier transition metals of groups 5 and 6 form ternary lithium nitrides with anti-fluorite-type structures (e.g. Li_7NbN_4, Li_7TaN_4) [72,73] also exhibiting additional lithium vacancies (e.g. Li_6MoN_4, Li_6WN_4; i.e. $Li_6\square MN_4$) [62]. Li_3N reacts with zirconium and hafnium to yield Li_2ZrN_2 and Li_2HfN_2, respectively. Both compounds have the anti-La_2O_3 structure [74–76]. Like α-Li_3N itself, the anti-fluorite and α-Li_3N type ternary compounds have aroused great interest in terms of their high Li^+ ion conductivity [77–81]. Both series of compounds are being extensively tested as anode materials in potential new Li batteries.

Li_3N reacts with p-block elements such as Al, Ga, Si, P to form ternary nitrides also crystallising with anti-fluorite superstructures (e.g. Li_3AlN_2, Li_3GaN_2, Li_5SiN_3, Li_7PN_4) [61,82]. Other compositions are also known, including, for example, $LiPN_2$ with the filled cristobalite structure [83] and $LiSi_2N_3$ and $LiGe_2N_3$ with wurtzite superstructures [84–86]. Lithium nitride reacts with boron to form Li_3BN_2 which exists in two forms, both containing linear $[NBN]^{3-}$ units [87,88]. Reaction chemistry with the lanthanides and actinides is sparse, although the compounds Li_2MN_2 (M = Ce, Th, U) with tetravalent metals exist with structures isotypic to $Li_2Zr(Hf)N_2$ [74,75].

Li_3N also reacts with lithium halides, LiX, at moderate temperatures (approximately 450–500°C) to form a variety of compounds with either layered or more complex 3-D structures. The former structures can be essentially described as intergrowths of Li_3N and LiX layers (or more accurately, $[Li_4N]^+$ and $[Li_yX_{y+1}]^-$ layers), including for example Li_4NCl and Li_5NCl_2 [89,90]. The latter nitride chloride also exists in a high temperature form with a Li_2O-type structure in which

nitrogen and chlorine are disordered. The compounds of Li, N and the heavier halides (X = Br, I), $Li_{3-2y}N_{1-y}X_y$, have structures composed of $Li_{3n+m}N_n^{m+}$ 3-D nets which in many cases are closely related to the Li–N arrangement in Li_3N. Examples include Li_5NBr_2, Li_6NBr_3, Li_6NI_3, Li_7N_2I and $Li_{10}N_3Br$ [91–94]. Similarly, Li_3N reacts with lithium hydride to yield Li_4NH with an ordered variant of the Li_2O structure [95]. The nitride hydride is also attainable via the decomposition of the amide in vacuuo. Li_4NH decomposes to the imide, Li_2NH plus either LiH or Li_3N when heated at approximately 400°C in hydrogen or nitrogen, respectively. By contrast, lithium nitride reacts with lanthanide and early transition metal halides in self-propagating solid state metathesis (SSM) reactions to yield the corresponding binary lanthanide or transition metal nitrides plus lithium halide [96,97]. These SSM reactions offer a rapid, low energy route to nanoparticular binary nitride materials.

2.1.2. β-and γ-Li_3N

Lithium nitride is also reported as existing in two other forms at increased pressure. Neither of these phases has been so extensively studied as α-Li_3N, to date, in terms of either crystal chemistry or physical properties. β-Li_3N was first observed in ^{7}Li-NMR experiments conducted on Li_3N at elevated pressures [98]. The pressure induced phase transition was observed to occur at 4.2 kbar at 300 K and although the new phase could not be structurally characterised, two inequivalent Li sites were identified with quadrupole coupling constants markedly different to those in α-Li_3N (406 and 164 kHz, respectively, as opposed to 582 ± 2 and 285 ± 2 kHz in α-Li_3N [49]). Interestingly spin–lattice relaxation and linewidth studies indicated a higher Li^+ mobility than in the α-form. Subsequently, independent powder diffraction studies identified the new phase as hexagonal with $c/a = 1.78$ (as opposed to 1.06 in α-Li_3N) [99,100]. Both studies measured the phase transition to occur at approximately 1 GPa. By inference, the new phase was characterised as of the Na_3As-type structure which agreed well with calculated diffraction data based on the arsenide as a model. β-Li_3N is thus isostructural with Li_3P (Fig. 3) and is consistent with the premise of applying a 'chemical pressure' by substitution of larger (an)ions. The structure of the β-phase retains certain key aspects of the α-structure, but here the Li–N layers switch from a composition [Li_2N] to [LiN] as nitrogen atoms are shifted from a simple hexagonal packing to hexagonal eutaxy. The immediate nitrogen coordination changes from hexagonal bipyramidal to trigonal bipyramidal. Each nitrogen, however, is further coordinated by a trigonal prism of more distant lithium atoms (at approximately 2.3 Å) creating an overall coordination geometry of a trigonal prism capped on all five faces. Optical absorption measurements in the region 1.85–2.30 eV show a shift of the absorption edge to higher energy with increasing pressure ($P < 0.6$ GPa). Beyond the phase transition, the absorption continues to increase, but little edge structure is evident [99].

Evidence for a third phase of lithium nitride, γ-Li_3N, was observed in depressurised samples subjected to pressures above 10 GPa [99]. The high pressure phase was characterised with a cubic face-centred unit cell, assumed to be isostructural

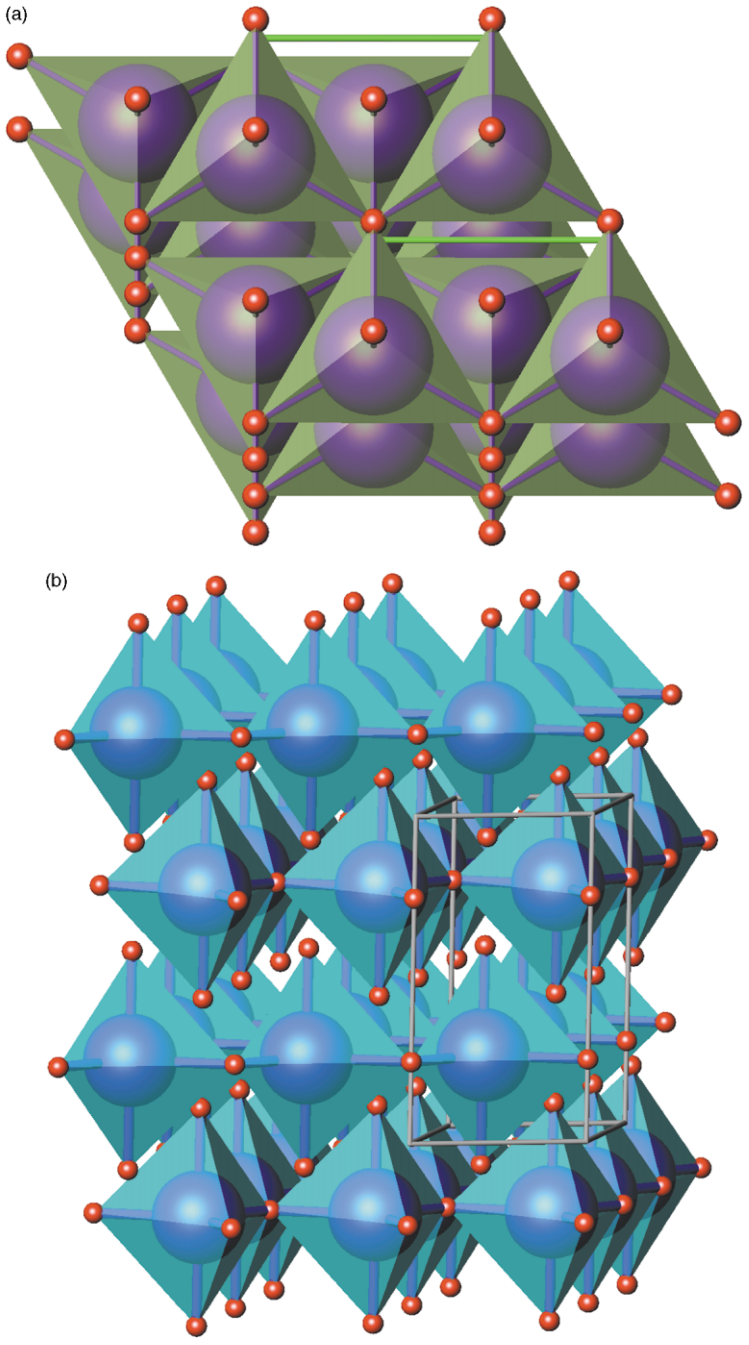

Fig. 3. Polyhedral representation of the structure of β-Li_3N with the Li_3P structure (a) viewed in the *ab* plane showing successive layers of corner sharing NLi_5 trigonal bipyramids; (b) showing packing of layers along the *c*-axis. Only the first coordination spheres of the N atoms are shown. Small spheres represent Li; large spheres within polyhedra represent N.

with Li_3Bi. Similar transformations between Na_3As and Li_3Bi structure-types are observed in other alkali metal pnictides such as K_3Bi [101] and Li_3Sb [102] and again this shows consistency between ideas of 'chemical' and physical pressure. Theoretical and energy dispersive X-ray diffraction studies of the Li–N system with increasing pressure confirmed the presence of β-Li_3N and the likely existence of γ-Li_3N at higher pressure [103]. In fact, the β-phase was observed experimentally as a minority phase at close to ambient pressure (the calculated phase transition reportedly exists at -1.1 GPa insinuating the Li_3Bi structure is the ground state for Li_3N) and no evidence for α-Li_3N was seen at the lowest applied pressure of 3 GPa. The suspected γ-phase, however, was not seen until a pressure of approximately 28 GPa.

2.2. Nitrides of the heavier alkali metals

Aside from Li_3N, the stabilities of the alkali metal binary nitrides are predicted to be low on the basis of their lattice energies. In fact, only sodium nitride, Na_3N, has a calculated heat of formation, ΔH, and extrapolated Gibbs free energy of formation, ΔG, that might suggest a thermodynamically (meta)stable compound (Fig. 4) [21,104]. This is also in line with the observed solubilities of nitrogen in the liquid alkali metals. Even in sodium, nitrogen is almost completely insoluble (6×10^{-11} mol l^{-1} atm^{-1}) and indicators suggest that nitrogen is dissolved as diatomic N_2 rather than as the anion N^{3-} as in liquid lithium [21,105]. Correspondingly, the solubility of the respective nominal nitride salt in sodium is also far lower than Li_3N in lithium [106,107].

The purported synthesis of sodium nitride has been reported under various extreme conditions, yet the compound remains ill-characterised. No binary compound can be prepared from direct reaction of the elements at temperatures up to

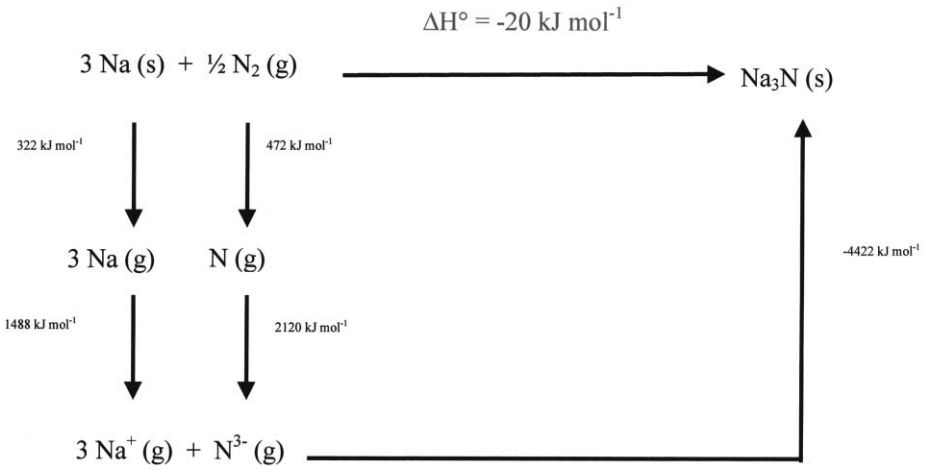

Fig. 4. Born–Haber cycle for the theoretical nitride, Na_3N [21].

800°C, even in the presence of an iron catalyst [104,108]. This useful property accounts for the use of nitrogen as a cover gas in liquid metal manipulation and in purifying the alkali metal. Coupled with the appreciable solubilities of lithium and the alkaline earth metals in sodium, this also allows use of liquid Na as a solvent for the preparation of the binary nitrides of these elements (as is highlighted in previous and subsequent sections). The successful synthesis of sodium nitride is only reportedly achieved using electrically activated nitrogen [109,110]. At low nitrogen pressures, the products of this sodium–nitrogen reaction are dependent on reaction time; over periods of up to 5 min the only observed product is Na_3N whereas over longer discharge durations both nitride and azide, NaN_3, are formed [104,109]. The identity of the nitride has never been reliably proven, however and no structural information exists. There is some speculation that nitride prepared in this way is in fact a mixture of the azide and sodium metal [12,111].

Reports of the synthesis of the other alkali metal nitrides are even more contentious. It is reported that the nitrides of potassium, rubidium and caesium can be synthesised following a similar procedure to the sodium case, reacting the metals with electrically activated nitrogen gas [104,110]. Here, the species appear to be even more short-lived; further reaction to the respective azides is far more rapid than for 'Na_3N' with KN_3, for example, detectable after only 30 s [110]. The black 'nitrides' are reportedly contaminated but, interestingly, reacted with hydrochloric acid to yield ammonia rather than hydrazoic acid supporting the existence of the N^{3-} anion (as opposed to azide) in the binary compounds [109]. Earlier unsubstantiated reports suggest that rubidium and caesium nitride can also be produced by the action of nitrogen gas on the corresponding hydrides [112]. Jansen and Schön recently used global optimisation techniques to calculate possible kinetically stable structures for these hypothetical compounds. A number of viable metastable modifications for Na_3N in particular were proposed [113].

3. Alkaline earth metal nitrides

By contrast to the nitride chemistry of the alkali metals, that of the alkaline earth metals is quite extensive and continues to grow with the periodic discovery of new binary, ternary and higher phases. However, none of these compounds have yet received the degree of attention of lithium nitride, for example. What is already fascinating is that clear trends in structure and bonding exist as one descends the group. Polytypes appear quite prevalent, although many of these compounds remain structurally ambiguous or uncharacterised. Arguably and intriguingly few of the compounds known to-date could be perceived as classically ionic solids.

3.1. Structural trends

As will be seen below, the compounds formed from the group 2 metals with nitrogen appear in many respects to become 'less ionic' with atomic number. Hence, perhaps surprisingly, as one descends the group one finds that structures become

less ionic with increasing metal electropositivity. Light alkaline earth metals such as beryllium and magnesium form exclusively salt-like compounds with only one, expected, stoichiometry. Barium, however, seemingly forms no such 'ionic' nitride but forms more than one partially metallic nitride with unexpected stoichiometries reflecting the cluster nature of the crystal chemistry. What is also becoming apparent, however, is that even in some of the ostensibly ionic compounds metals are coordinatively unsaturated to the anion, N^{3-}, and make up the first coordination sphere by bonding to neighbouring metals. Alternatively the metal–nitrogen bonds themselves may be regarded as being of significant covalent character. Both crystal and electronic structure studies are gradually beginning to illuminate the full importance of these interactions.

3.2. 'Ionic' nitrides

3.2.1. Beryllium nitride

The lighter alkaline earth metals form binary nitrides which might be termed, nominally at least, ionic. Beryllium forms the nitride, Be_3N_2 in two known polymorphs with a phase transition at approximately 1400°C [114]. The nitride subsequently vaporises congruently to Be and N_2 between 1640 and 1960°C [115]. The low temperature α-form is readily formed either by the action of nitrogen or ammonia on beryllium metal [115,116] at ambient pressure. The formation of the nitride is accelerated using ammonia under supercritical conditions [117]. Alternative syntheses of this form of Be_3N_2 also include the low temperature reaction of Be metal with NH_4Cl followed by brief annealing at higher temperature [118]. The resulting white solid crystallises with the cubic anti-bixbyite structure (Fig. 5), in which each beryllium atom is tetrahedrally coordinated to nitrogen [116]. Conversely, each nitrogen atom is octahedrally coordinated to beryllium. The higher temperature β-form, however, adopts a hexagonal structure in which beryllium atoms occupy interstitial sites within close packed nitrogen layers of sequence …HCHCHC… The original model for the placement of these interstitial beryllium atoms, yielded two tetrahedrally coordinated Be atoms and one in a trigonal planar position within an H-type nitrogen layer. This thus creates a Be layer sequence …CCHCCH… Subsequent refinement of the crystal structure revealed the three coordinate Be position to be vacant and replaced this Be atom in a half-filled tetrahedral site (Fig. 6). Thus, three of the four possible tetrahedral sites in the …HCHCHC… anion sublattice are occupied and nitrogen atoms are octahedrally coordinated in this structure. Ab initio Hartree–Fock calculations demonstrate that β-Be_3N_2 is a wide band gap semiconductor with an indirect gap of 12.5 eV and upper regions of the valence band formed mainly from N and Be p orbitals [119]. These calculations also indicate that the nitride constitutes a hard material (bulk modulus of 2.61 Mbar) and that, interestingly, the Be–N bonds possess significant covalent character.

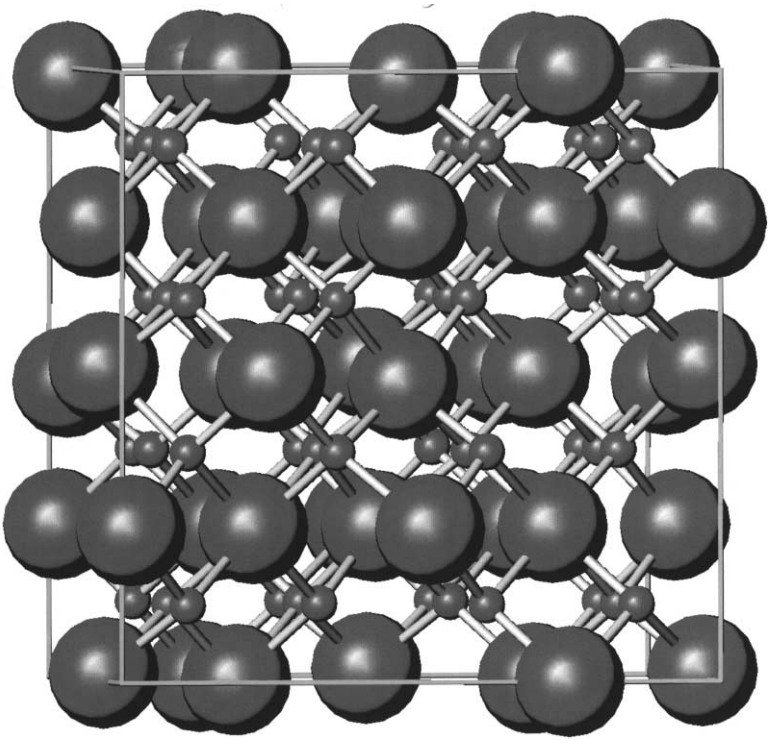

Fig. 5. Anti-bixbyite structure of α-Be_3N_2. Be is coordinated to N in a tetrahedral geometry. Small spheres depict Be, large spheres depict N.

3.2.2. Magnesium nitride

Magnesium nitride can be prepared in similar ways to Be_3N_2 either by reaction of finely divided magnesium metal with gaseous nitrogen or ammonia [116,120–122]. The solubility of magnesium in sodium [123] can also be exploited to obtain highly crystalline, phase-pure nitride by reacting sodium–solvated magnesium metal with nitrogen followed by vacuum distillation [124]. Synthesis is also reported from reaction of magnesium hydride with flowing nitrogen [125]; a route which recent studies have shown yields nanometric size nitride particles [126]. Sub-micrometer scale Mg_3N_2 is also attainable by low pressure CVD techniques via reaction of Mg vapour with N_2/NH_3 gas mixtures [127]. Three polymorphs of Mg_3N_2 were originally reported at ambient pressure with phase transitions at 550°C (α–β) and 780°C (β–γ), yet the reported energy differences between polymorphs were small and none of the phases were characterised [120].

The only substantiated form of Mg_3N_2 at ambient pressure crystallises with the anti-bixbyite structure isostructural to α-Be_3N_2 [128]. The structure of Mg_3N_2 has been more recently refined by powder neutron diffraction confirming the earlier representation but also emphasising the irregular tetrahedral geometry around the magnesium atoms [129]. Further analysis has also been performed by infra red (IR)

and Raman spectroscopy which revealed spectra similar in appearance to the isostructural rare earth sesquioxides [130]. The coordination environment around the magnesium atoms is unusually low and implies Mg is coordinatively unsaturated. Bond valence calculations confirm this and suggest bonding in Mg_3N_2 is not purely ionic. The electronic structure of Mg_3N_2 has been calculated using the local spherical wave (LSW) approach [131]. The results of the ab initio calculations describe Mg_3N_2 as a semiconductor with a band structure in which the valence band is approximately 4.4 eV wide and composed mainly of N 2*p* states. The conduction band consists mainly of Mg 3*s* and N 3*s* states. The calculated direct band gap of 1.1 eV is smaller than that obtained from optical diffusivity experiments (2.8 eV).

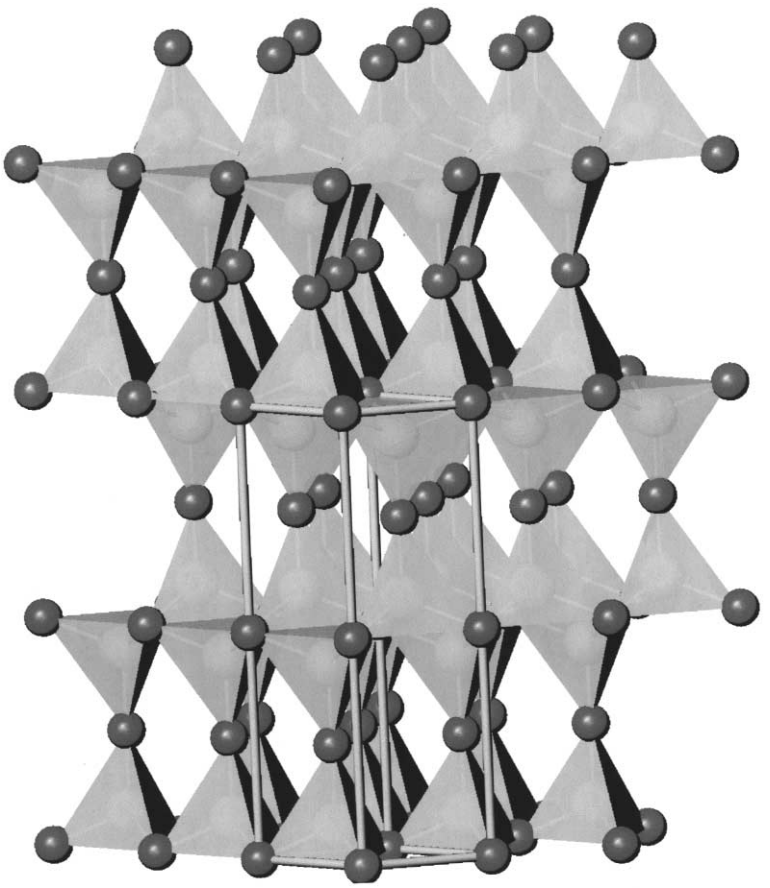

Fig. 6. Structure of β-Be_3N_2, showing coordination geometry around Be. Double layers of edge-sharing inverted BeN_4 tetrahedra are linked along the *c* direction by the vertices. Three of the four tetrahedral sites in the structure are filled by Be and one of these is half occupied. Small spheres at the corners of tetrahedra represent N, medium spheres within tetrahedra represent Be.

The existence of other polymorphs of Mg_3N_2 at higher pressures remains to be corroborated. Bradley et al. discovered the presence of additional reflections in in situ powder X-ray patterns of Mg_3N_2 collected between 10 and 90 kbar, but the observations were not reproducible [125]. More recent studies over a pressure–temperature regime of up to 1900 K and 1.5–9.0 GPa lead to a phase diagram in which six solid phases apparently exist [132]. By extrapolation of the phase boundaries to ambient pressure, phases II and III are proposed to be the elusive β-and γ-polymorphs reported several decades earlier [120]. However, since all the transformations within the $P–T$ phase diagram were observed to be reversible, none of the additional five phases of Mg_3N_2 were characterised. Indeed, MgO was found to be an impurity after the experiments inevitably shedding some doubt as to the identity of the high pressure nitride phases.

In similarity to Be_3N_2, the reaction chemistry of Mg_3N_2 is currently somewhat limited. Both compounds react with silicon nitride to yield the corresponding $A^{II}SiN_2$ phase [133–136] with wurtzite-related structures. Magnesium nitride also reacts with other main group nitrides, producing for example, Mg_2PN_3 [137,138] and $MgGeN_2$ [135] and Mg_3GaN_3 [139]. Magnesium nitride reacts with magnesium dihalides, MgX_2 leading to the corresponding nitride halides, Mg_2NX (X = F, Cl, Br, I) [140,141]. Importantly, Mg_3N_2 has been shown to catalyse the formation of cubic boron nitride (cBN) at high pressures from the hexagonal form (hBN) [142]. Magnesium nitride itself is highly reactive to water. Original studies determined that hydrolysis to $Mg(OH)_2$ and NH_3 occurs within 5 min in liquid water but is much slower under the 'dry' conditions of atmospheric water vapour at 22°C [122]. The kinetics of the atmospheric hydrolysis have been followed by in situ FT-IR and Raman spectroscopy illustrating that $Mg(OH)_2$ formation is 'instantaneous' on air exposure (within 30 s) and occurs via a 3-D diffusion process [130].

3.2.3. Calcium nitrides

In contrast to beryllium and magnesium, the nitride chemistry of calcium is relatively rich both in terms of the binary compounds formed in the Ca–N system and in the ensuing reaction chemistry of these nitrides. Calcium is unique in that is the only group 2 element to unequivocally form both 'ionic nitrides' and subnitrides. The latter compounds will be described in Section 3.3. Recent findings have shown, however, that many of the seemingly binary compounds previously identified in this system have their origins elsewhere.

Calcium nitride, Ca_3N_2, reportedly exists in three forms. The α-form remains the only one of these polymorphs that has been extensively characterised. Red-brown α-Ca_3N_2 is formed by the direct action of nitrogen on purified calcium metal between approximately 650 and 1150°C [116] or at reduced temperatures using sodium as a solvent for the alkaline earth metal [143]. The original study identified α-Ca_3N_2 as being isostructural with the anti-bixbyite structure of Mg_3P_2 and therefore also with α-Be_3N_2 and Mg_3N_2 [116]. Debye Scherrer X-ray diffraction data provided a more complete, but still fairly approximate, representation of the structure several decades later [144]. Subsequent single crystal and powder X-ray diffraction studies have revealed the tetrahedral coordination around the Ca atoms

to nitrogen to be considerably more distorted than in the first idealised structure solution [130,145,146]. This highly irregular, coordinatively unsaturated environment has since been confirmed by powder neutron diffraction and EXAFS experiments and resembles the metal coordination in the other $A_3^{II}N_2$ compounds with essentially one short and three long metal–nitrogen bonds (Fig. 7) [147]. Bond valence calculations for α-Ca_3N_2 yield a low Ca oxidation state (in similarity to Mg in Mg_3N_2), suggesting bonding may not be purely ionic.

α-Ca_3N_2 reacts readily with water, hydrolysing completely in liquid water within 5 min and undergoing complete reaction with atmospheric water to $Ca(OH)_2$ and ammonia within 5 h at 22°C [122]. In this respect, its reactivity to water is enhanced relative to Mg_3N_2 as confirmed by in situ FT-IR and Raman experiments [130]. The air sensitivity of α-Ca_3N_2 has almost certainly affected reliable measurements of its electrical properties as reported in the literature. Studies indicate that the electrical conductivity is heavily dependent on the gaseous environment under which the measurements were performed. Conductivity drops in a nitrogen–hydrogen mixture as Ca_2NH is apparently formed. Doping α-Ca_3N_2 with LaN seemingly increases the ionic contribution to the total conductivity. Significant wt.% values for oxygen, however, were measured for most tested samples [148–150].

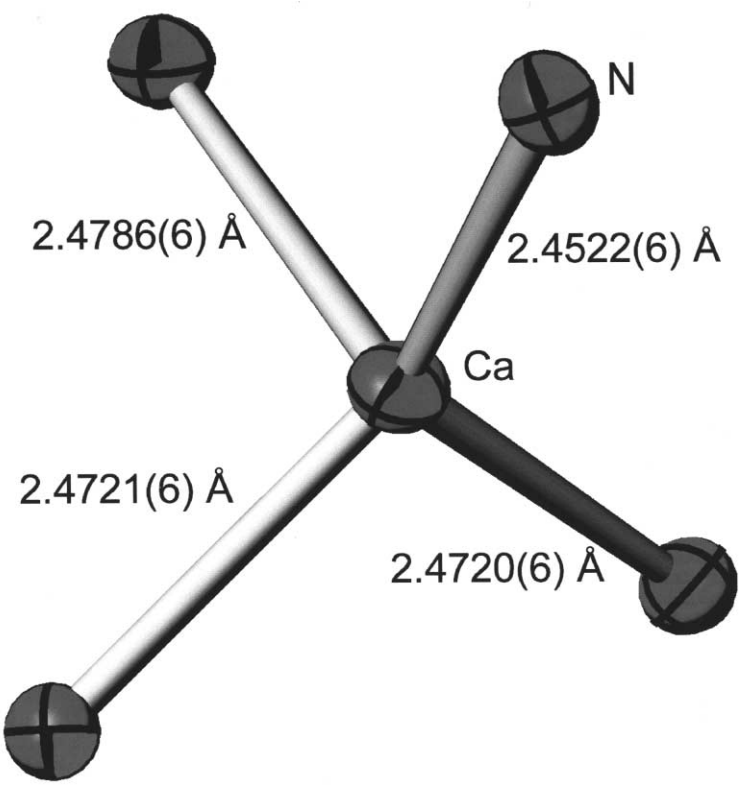

Fig. 7. Distorted, coordinatively-unsaturated tetrahedral coordination geometry of Ca in Ca_3N_2 [147].

The two other reported forms of Ca_3N_2 are formed at lower and higher temperatures than the α-polymorph. The yellow, high temperature, γ-form was observed when distilled calcium was heated under purified nitrogen at temperatures above 1050°C followed by rapid cooling [151]. The orthorhombic nitride was observed to transform rapidly to cubic α-Ca_3N_2 when heated to 900°C, but the reverse transition was never observed. More recent evidence, however, has revealed the likely true identity of the high temperature phase as one of two new nitride cyanamides, $Ca_4N_2(CN_2)$ (the other being $Ca_{11}N_6(CN_2)_2$) [146,152]. The orthorhombic structure and ensuing X-ray powder pattern of the carbon-containing compound derived from single crystal data is remarkably similar to that observed for 'γ-Ca_3N_2' and both compounds have the same coloration. The presence of cyanamide ions in $Ca_4N_2(CN_2)$ was confirmed by IR and Raman spectroscopy and the origin of the unexpected carbon in these syntheses is identified as an impurity from container materials (e.g. steel) or as an impurity in the calcium itself (although allegedly of 99.99 + % purity). Direct syntheses of the nitride cyanamide from Ca_3N_2, NaN_3 and degassed graphite led to the same products, $Ca_4N_2(CN_2)$ and $Ca_{11}N_6(CN_2)_2$ (further details of this latter compound follow below). The black, low temperature β-form of Ca_3N_2 forms from the reaction of Ca with nitrogen at temperatures around 350°C [153,154], although nitrogen uptake is first observed at approximately 200°C [155]. The β-form remains poorly characterised but powder patterns have been tentatively indexed on a pseudo-hexagonal unit cell [154]. The high observed density of the β-phase led Bradley et al. to their belief that it might be stabilised at high pressures [125]. They observed that a predominantly black sample of nitride was obtained after heating α-Ca_3N_2 to 1800°C at 46 kbar for 8.5 min followed by rapid quenching. The product gave an X-ray powder pattern that could be indexed on an orthorhombic unit cell ($a = 5.625$ Å, $b = 11.40$ Å, $c = 13.61$ Å). Recent synthesis of a phase resembling β-Ca_3N_2 was performed by reacting Ca metal with NaN_3 at approximately 300°C and although direct evidence of sodium inclusion is not yet forthcoming, there is a suspicion that the compound may be a subnitride with parallels to the Na–Ba–N system detailed in Section 3.3 [146]. The observed powder pattern for this phase, however, is quite different to that obtained by Bradley et al.

Two other binary compounds of calcium with nitrogen have been reported, the pernitride Ca_3N_4 and the compound of composition $Ca_{11}N_8$. The latter composition was originally observed as a crystalline deposit in samples of Ca_3N_2 heated under nitrogen to 1050°C. Single crystal X-ray diffraction of this by-product revealed a tetragonal structure containing two sorts of infinite Ca–N chains, $(Ca_3N_2)_n$ and $(Ca_4N_3)_n$ [156]. The resulting refinement however, was relatively poor with some anomalously large Ca–N distances reported. The probable true nature of the nitride has since been revealed as the nitride cyanamide $Ca_{11}N_6(CN_2)_2$ [152]. As with $Ca_4N_2(CN_2)$ above, the source of carbon would originally seem to be have been impurities in the calcium itself and/or contamination from the container material. Refinement of one of the nitrogen positions as a triatomic cyanamide unit, led to a solution with good residuals and a crystal structure with more reasonable calcium/nitrogen environments. The existence of the cyanamide anion was again

also confirmed by IR and Raman spectroscopy. Interestingly, attempts to synthesise bulk, phase pure samples of each of the nitride cyanamide phases from Ca_3N_2, NaN_3 and C always result in multiphase ($Ca_{11}N_6(CN_2)_2$ and $Ca_4N_2(CN_2)$) products. Similar results were obtained independently from direct reaction of Ca_3N_2 and $Ca(CN_2)$ at elevated temperatures [157]. Refinement of powder neutron diffraction data of these latter biphasic products led to structural models in good agreement with the X-ray data (Fig. 8) and confirmed the identity of the triatomic units as $(CN_2)^{2-}$. The pernitride, black Ca_3N_4, was originally reported by Hartmann et al. in 1934 and was synthesised by the decomposition of the amide under high vacuum [158]. The product was neither isolated nor characterised, however. Subsequent

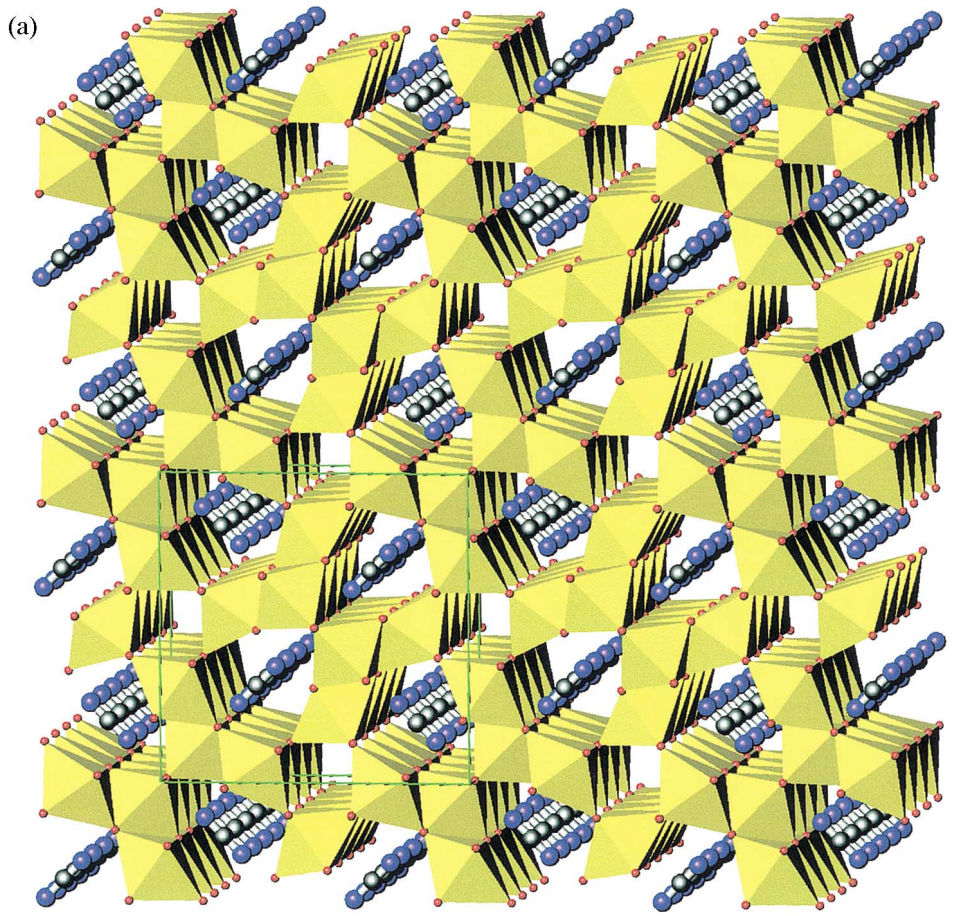

Fig. 8. Crystal structures of the calcium nitride cyanamides (a) $Ca_{11}N_6(CN_2)_2$ and (b) $Ca_4N_2(CN_2)$ with 3-D Ca–N networks built up from NCa_6 edge and vertex sharing octahedral units. Cyanamide ions sit within channels in the 3-D framework. Small black spheres represent C, small blue spheres represent N, and small red/orange spheres represent Ca.

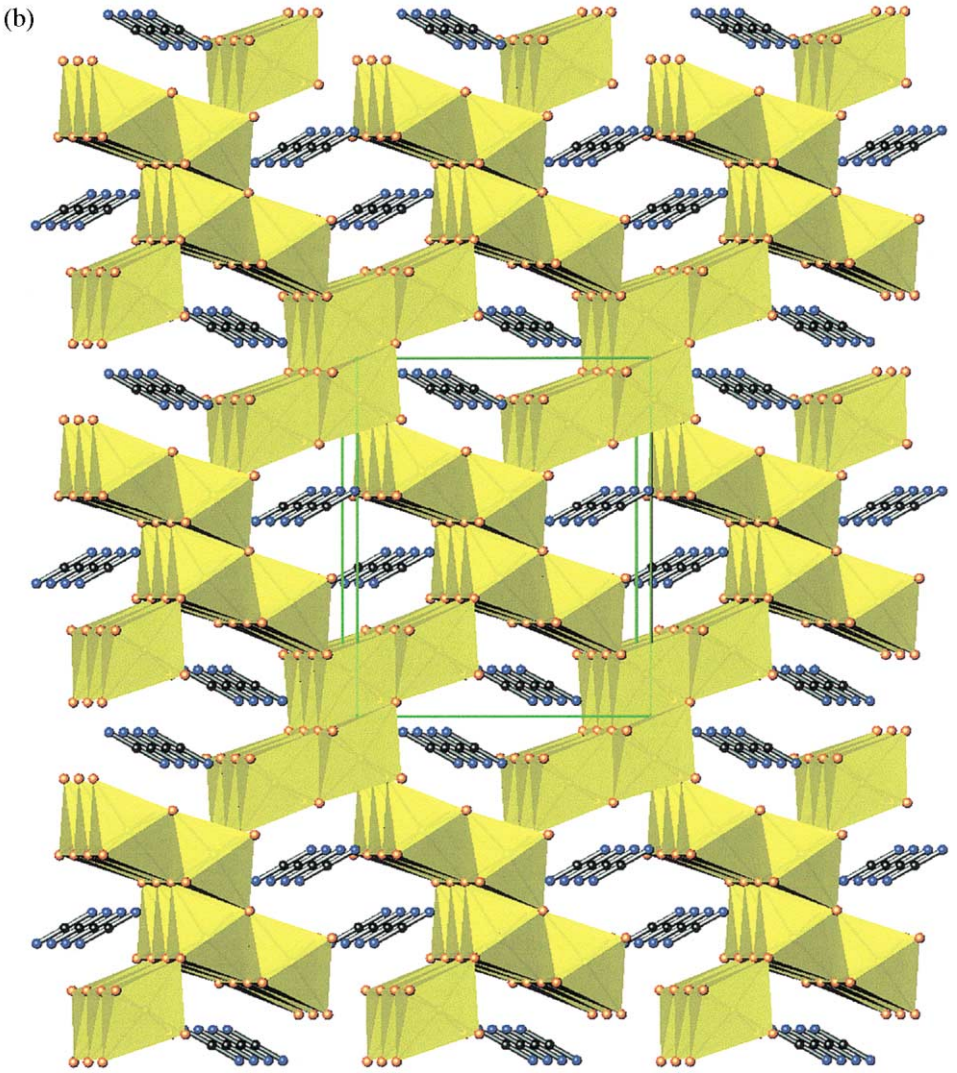

Fig. 8. (*Continued*)

preparation of the pernitride was performed 30 years later by the controlled decomposition of calcium azide in dried organic solvents (decalin, xylene and tetralin were all found to be successful) [159]. This reaction yielded the pernitride plus nitrogen gas. Further heating of the highly air sensitive pernitride under nitrogen at 250°C yielded Ca_3N_2 plus further nitrogen. Although the composition was determined by analyses, no structural characterisation of Ca_3N_4 was performed. Although further attention has been directed towards Ca_3N_4, including suggestions that it is deficient in nitrogen and is paramagnetic at room temperature [160–162], it remains a poorly defined compound.

The reaction chemistry of the best-defined 'ionic' calcium nitride, α-Ca_3N_2, is extensive compared with the lighter group 2 binary nitrides, yielding a large variety of ternary and higher compounds with main group and transition elements alike. The full range of compounds will not be considered here and a cross-section of transition metal compounds can be found, for example, in [1,2,12] among others. Calcium nitride reacts with p-block binary nitrides to produce a host of compounds with structures of various dimensionality. Compounds with phosphorus and silicon are dominated by the $P(Si)N_4$ tetrahedral unit, isolated or linked predominantly by vertices to form chain, layer or 3-D network structures [4,163–165]. Similar units are prevalent in ternary gallium and germanium compounds (e.g. $Ca_3[Ga_2N_4]$ [166], $Ca_5[(GeN_3)_2]$ [167]) although lower coordination numbers are also observed in the nitridogermanates (e.g. Ca_2GeN_2 containing linear isolated $[GeN_2]$ units [167]). Like Mg_3N_2, calcium forms a number of nitride halide compounds, A^{II}_2NX (and also the nitride hydride, Ca_2NH) with structures dependent on the size of the halide. Ca_2NH and Ca_2NF possess ordered and disordered rocksalt type structures, respectively [168–171] whereas with the heavier halides the Ca_2NX compounds have layered structures of either α-$NaFeO_2$ (X = Cl, Br) or $RbScO_2$-type (X = I) [172–175]. In parallels with Mg_3N_2, α-Ca_3N_2 also acts as a flux and modifier in the preparation of cBN from hexagonal boron nitride [176]. The role of α-Ca_3N_2 here however, appears to be not so much catalytic but more in determining crystal size and morphology.

3.2.4. Other compositions

Whereas, as will be seen below, the subnitride chemistry of strontium and barium is well defined, the existence of 'ionic' compounds, particularly those of expected composition $A^{II}_3N_2$, is dubious. Sr_3N_2 was reported in 1923 [177] and later described in more detail as a product of the reaction of purified strontium metal with dry nitrogen [116,178]. At this time it was noted that the powder X-ray diffraction pattern of the nitride could not be indexed by analogy to the cubic anti-bixbyite structures of Be_3N_2, Mg_3N_2 and Ca_3N_2. In later studies, emphasis was made that the ideal $A^{II}_3N_2$ composition was never reached and that the compounds were always nitrogen deficient (e.g. Sr:N = 1:0.333 and Sr:N = 1:0.63-the latter was nominally labelled Sr_8N_5 and tentatively indexed on a monoclinic unit cell) [179,180]. The resulting products were never incontrovertibly characterised. With the later isolation and successful indexing of the subnitride Sr_2N (as detailed in Section 3.3) [181], a reassessment of Sr_3N_2 led to the assertion that the compound was in reality a mixture of Sr_2N and the controversial compound 'SrN' [182]. Others claimed the true identity of Sr_3N_2 was a nitride hydride with variable composition $Sr_3N_{2-x}H_y$ where hydrogen contamination emanates from impurities in the alkaline earth metal itself [183]. Sr_3N_2 has yet to be isolated and characterised beyond reasonable doubt. 'SrN', meanwhile, has been revealed to be almost certainly the imide SrNH [158] or the less well characterised oxynitride (hydride) $Sr(ON)(H_y)$ [184]. Both these compounds have the same colour (black) and same crystal structure (rocksalt) as the purported nitride. The imide SrNH is synthesised by the reaction of Sr_2N with hydrogen which also yields SrH_2 as a secondary

product [185]. Interestingly, both SrNH and Sr_2NH are obtained from the reaction of Sr metal with a mixture of hydrogen and nitrogen gas [186] while reaction of strontium with ammonia produces a distorted modification of SrNH (β-SrNH crystallising in space group *Pnma* with ordered H positions) which transforms to the rocksalt structure of α-SrNH above 750°C [187].

Barium nitride, Ba_3N_2 has been the subject of rigorous scrutiny less often than Sr_3N_2 but its existence appears only slightly less debatable. Early studies, as with Sr_3N_2, identified the product of the nitridation of barium metal only on the basis of chemical analysis [177,178]. The compound was also observed to be obtained from the decomposition of the azide, $Ba(N_3)_2$, but no sound characterisation was performed [188]. Attempts to characterise the nitride have suffered chiefly from the reported recurrent poor crystallinity of the compound and powder X-ray diffraction patterns, for example, are generally only in loose agreement [12,188–190]. The nitride has been indexed on the basis of at least two hexagonal unit cells [160,191] while the only single crystal study describes a rocksalt structure in which the nitrogen position is partially occupied to give a composition $Ba_3N_{2.1(1)}$ [190]. Although analysis of the nitride in this latter study confirms a Ba:N ratio close to 3:2, the structure ostensibly resembles the imide, BaNH [192]. Both barium and strontium pernitrides, Ba_3N_4 and Sr_3N_4, respectively, reputedly exist but as with Ca_3N_4, concrete evidence of their identity is not forthcoming and any detailed characterisation remains to be performed [158–162]. Another pernitride of barium, BaN_2, has also been reported but these reports have never been substantiated [193]. Similarly Ba_2N_2, containing the unusual N_2^{4-} anion, was claimed to be an alternative product of the reaction of barium metal and nitrogen but no meaningful characterisation of the compound exists [191].

3.3. Binary and higher subnitrides

Clues as to the potentially rich chemistry of the alkaline earth subnitrides were probably first forthcoming from studies, chiefly in the 1970's, of the solubility of the group 2 metals in sodium and the subsequent dissolution of nitrogen in these alkali metal–alkaline earth metal melts [194–200]. First reports of nitrogen deficient phases in A^{II}–N systems, however, predated these studies with the observation of alkaline earth metal compounds of composition A_2N (A = Ca, Sr, Ba) [116,201–204]. Sr_2N and Ba_2N were obtained by heating the respective nominal 'A_3N_2' nitrides in vacuuo at temperatures from 450 to 500°C and characterised on the basis of analyses [201]. The first structure determination of an A_2N subnitride was achieved from a crystal of Ca_2N, although the conditions of synthesis and crystal growth were not specified [203,204]. Although in some senses approximate, the structure determination provided a model that was later proved fundamentally correct [205]. The compound adopts an anti-variant of the $CdCl_2$ structure in which nitrogen is octahedrally coordinated to six calcium atoms and calcium is bonded to three nitrogen atoms in a pyramidal geometry (essentially an 'incomplete' or 'half-fulfilled' octahedron). The NCa_6 octahedra link by edges to form nominally $[NCa_2]^+$ layers stacked along the crystallographic *c*-axis, leaving large van der

Waals-type gaps between these N–Ca slabs (Fig. 9). The layers in the compound were proposed to be essentially ionic with the excess electron per formula unit located within the van der Waals gaps (i.e. $(Ca^{2+})_2\ N^{3-} \bullet e^-$). Earlier conductivity measurements on Ba_2N had categorised it as a 'poor metal' [201] and the preliminary measurements performed at the time on powders of Ca_2N placed it in the same category [203,204]. It was suggested that on the basis of structural arguments, these compounds were 2-D metals with conduction along *c* (perpendicular to layers) probably orders of magnitude poorer than that parallel to layers.

Sr_2N was identified as isostructural shortly afterwards [181]. Debates in the literature then ensued as to the true nature of the A_2N compounds and the purported unintentional hydride intercalation (from impurities in the alkaline earth metals, for example) allegedly needed to obtain charge neutral solids. In this respect Brice et al. claimed that Ca_2N, Sr_2N and Ba_2N were non-existent and were in reality the nitride hydrides A_2NH_y [184]. The veracity of the A_2N formalism was confirmed 15 years later for Sr_2N through a systematic synthetic and analytical investigation followed by characterisation via powder neutron diffraction [206]. The subnitride was prepared by the reaction of the purified elements at 750°C. The study demonstrated the absence of hydride within the Sr_2N structure and that powders of the nitride were Pauli paramagnetic metallic conductors. Similar more recent powder neutron diffraction studies have confirmed that Ca_2N is of a like A_2N composition and anti-$CdCl_2$ structure and has electronic properties of the same order [205]. Interestingly, however, the ratios of $[NA_2]^+$ layer thickness to

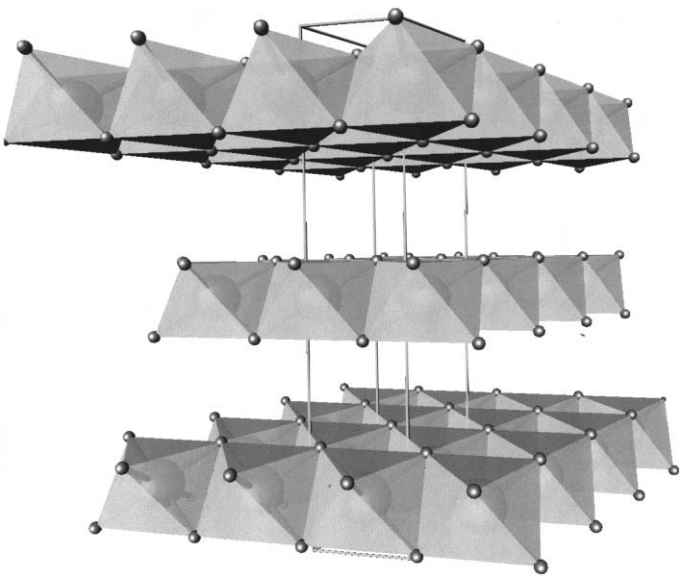

Fig. 9. The 2-D anti-$CdCl_2$ structure of Ca_2N (Sr_2N, Ba_2N). Layers of edge-sharing NCa_6 (NSr_6, NBa_6) octahedra run parallel to the *ab* plane, stacked along *z*. Van der Waals-type gaps containing free electrons exist between positively charged $[A_2N]^+$ slabs.

interlayer spacing are in closer agreement to Sr_2N than the original study of Ca_2N with a concomitant increase in *c* parameter. This might suggest that the originally reported Ca_2N has a different composition from that nominally proposed (which was not determined analytically in that study). Ca_2N was synthesised via reduction of Ca_3N_2 or by reaction of nitrogen gas with Ca dissolved in liquid sodium within a narrow temperature range. Although no structure refinements of Ba_2N exist in the open literature, independent single crystal X-ray diffraction experiments provide an isostructural model with the other A_2N nitrides [190,207]. Ba_2N appears the most difficult of the A_2N nitrides to crystallise, certainly in terms of obtaining crystals that yield reliable diffraction data. Although no detailed decomposition studies have been performed, the air sensitivity of all the A_2N subnitrides is extreme with samples producing the respective alkaline earth hydroxide and ammonia within seconds of air exposure.

The structure, bonding and electronic properties of the A_2N subnitrides have been compared with other excess electron compounds such as Ag_2F. The latter compound crystallises with the layered anti-CdI_2 structure and is a 3-D metal and a superconductor at low temperature [208,209]. The crucial difference structurally between the fluoride and the subnitride is the contrast in metal–metal bonding between and within $[XM_2]^+$ layers and hence the difference between layer thickness and interlayer spacing. In Ag_2F, the Ag–Ag interlayer distances are shorter than the intralayer separations, whereas in the A_2N compounds the converse is true. Anisotropic electrical properties are predicted for the subnitrides as the 2-D electron gas is constrained between ionic slabs (the cores of each being a layer of N^{3-} anions). Although values of the conductivity for powdered nitride samples are not high and lack consistency, directionally dependent properties (e.g. of crystals) are yet to be measured. The electronic structures of the A_2N compounds have been investigated experimentally by ultraviolet photoelectron spectroscopy (UPES) and theoretically by density functional theory (DFT) calculations [210,211]. There is some discrepancy in the results of these measurements and calculations but all data support the premise of ionic layers within the structures of these compounds. Linear Muffin-tin orbital atomic sphere approximation (LMTO-ASA) calculations loosely support UPES data describing N 2*p* DOS with single or double peaks at low binding energies (ca. 2.5 eV) and diffuse 'tails' to higher binding energies [210]. Although the calculated structure of the N 2*p* DOS is different using pseudo-potential (PP) and LSW methods, the band width (approximately 2 eV) is essentially the same and the A_2N compounds can be described in all cases as metals [211]. Linear augmented plane wave (LAPW) methods have been used to calculate the band structures of the related phases, Sr_2NH and Ba_2NH where hydrides ions now fully occupy the interplanar positions in the A_2N structure (α-$NaFeO_2$-type) [212]. The band structures of the nitride hydrides are in many ways similar, with the N 2*p* band again approximately 2 eV wide. A calculated direct band gap now exists, however, with a value of 1.6 eV as opposed to a direct gap of approximately 3 eV and an indirect gap of 2.5 eV measured for Sr_2NH [186]. Hence these layered materials become more insulating following hydride intercalation.

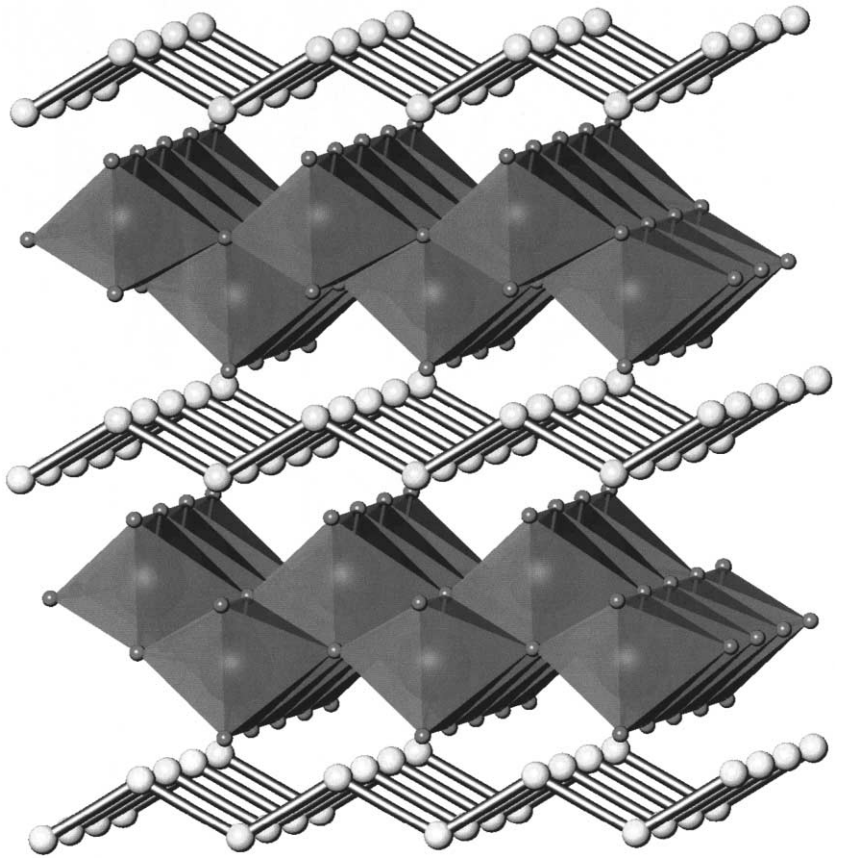

Fig. 10. Orthorhombic structure of Ca_2AuN. Infinite zig-zag chains of Au^- ions (medium spheres) alternate with corrugated $[Ca_2N]^+$ layers of edge-sharing NCa_6 octahedra along the *b*-axis.

The reaction chemistry of the A_2N compounds is varied and intriguing. Halides can be intercalated within Sr_2N and Ba_2N to yield the corresponding A_2NX (X = F, Cl, Br) compounds which apparently retain a 2-D structure (unlike Ca–N–X systems described in Section 3.2.3 where the dimensionality of the ternary compound appears more anion sensitive) [213]. Potentially even more interesting, however, are the prospects of adding or intercalating more complex species such as metals or complex metallate anions. The principle of metal addition is well tried in 1-D systems, as will be seen below for Ba–N compounds, but in the 2-D case there is only one example, Ca_2NAu, to date [214]. The nitride auride is synthesised from Ca_3N_2 and gold foil at 820°C under high nitrogen pressures (typically 200 bar upwards). Here the framework of slabs of NCa_6 edge-sharing octahedra found in Ca_2N buckles and shears to accommodate alternating layers of zig-zag chains of gold atoms (Fig. 10). Nitridometallate anions have also been accommodated in Ca_2N-related frameworks in the Ca_6MN_5 compounds (M = Mn, Fe, Ga) [215,216].

Layers of edge sharing NCa_6 octahedra here contain holes (i.e. 'pores') where nitrogen has effectively been removed. This creates $[NCa_3]^{3+}$ layers and the means by which the highly charged, but geometrically flat, trigonal planar $[MN_3]^{6-}$ anions can be inserted (Fig. 11).

The A_6N octahedron that constitutes the component of the edge-sharing layers in the 2-D A_2N materials is also the fundamental building block in a vast range of 0- and 1-D binary and higher subnitrides that have been discovered over the last decade. These unique cluster compounds have been synthesised and characterised almost exclusively by Simon and co-workers and in-depth accounts of this work can be found in [10,11]. With parallels to the chemistry of the alkali metal suboxides [217,218], suggestions that alkaline earth subnitrides might exhibit a similar chemistry originated from earlier studies of alkali metal–alkaline earth metal–nitrogen ternary systems. It was discovered by following both solubility and electrical resistivity of solutions that when nitrogen is added to barium dissolved in liquid sodium, a number of Ba-rich species are apparently formed in solution prior to the precipitation of thermodynamically stable Ba_2N at higher N concentrations [196–198]. It was not until much later that the full significance of these results was appreciated. It had been previously proposed that sodium itself entered the solva-

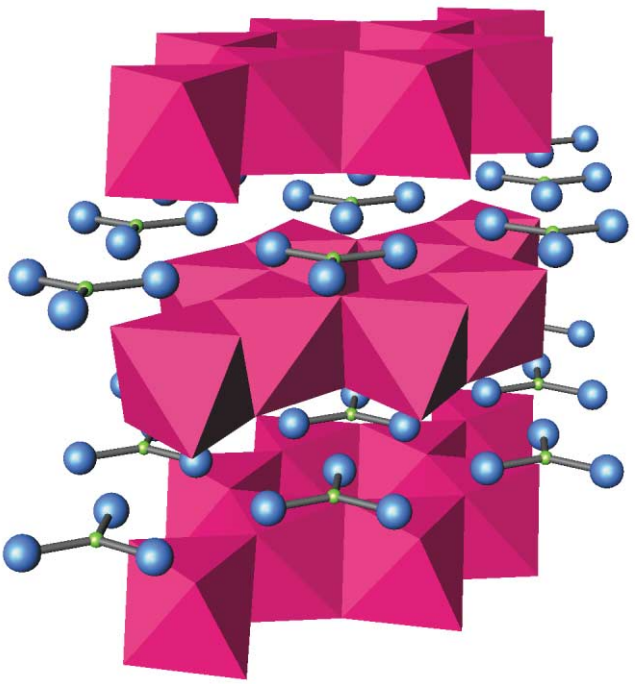

Fig. 11. Structure of Ca_6MnN_5. Discrete trigonal planar anions $[MnN_3]^{6-}$ are sandwiched between $[Ca_3N]^{3+}$ layers of NCa_6 edge-sharing octahedra such that alternating layers of the Mn–N triangles are rotated 180° in the *ab* plane relative to preceding and following Mn/N layers. Small green spheres and large blue spheres represent Mn and N, respectively.

tion shell of the N^{3-} anions in solution as the nitrogen concentration exceeded a Ba:N 4:1 ratio [197]. As this process occurs the solvation of N^{3-} decreases and Ba_2N is the precipitation product.

In fact, the resulting barium-rich solid species, Na–Ba–N, have structures in which N^{3-} bonds exclusively to the alkaline earth metal and sodium metal bonds exclusively to A^{2+}. The simplest of the Na–Ba–N subnitrides form the family Na_xBa_3N ($x = 0$, 1, 5) and are shown in Fig. 12 [219–222]. Here the NBa_6 octahedra form the common motif of face sharing NBa_3 (i.e. $^{1}_{\infty}[NBa_{6/2}]$) chains. When x is non-zero, these chains are interspersed by sodium atoms and hence, effectively, 1-D channels of the ionic salt are suspended within a metallic matrix. In each of the family members, therefore, insulating ionic wires composed of N–Ba ionic bonds are held together within a conducting bulk by Na–Ba metallic bonds. The existence of the $x = 0$ compound Ba_3N, however, illustrates that the sodium matrix is not necessarily required to hold these chains together to yield a stable solid and that this sodium-free compound might, therefore, be formalised $(Ba^{2+})_3$-$N^{3-} \bullet (3e^-)$ with free electrons located between insulating $[Ba_3N]^{3+}$ cores [222]. That the Ba–Ba distances between chains are larger in Ba_3N than in Ba metal (and also with the isostructural excess electron compound Cs_3O vs. Cs [223]) is explained in terms of the confinement of the electron gas outside the areas of concentrated negative charge and the release of this pressure through expansion of the Ba metallic sublattice. The electronic structures of the Na_xBa_3N compounds have been investigated by UPES measurements and LMTO–ASA calculations [210]. As expected the subnitrides are metallic with rather similar DOS in which mixing of metal and nitrogen orbitals is small. In each case the N 2*p* DOS is narrow in energy (approximately 0.2 eV) and is shifted by 0.2 eV to higher binding energy in the $x = 5$ compound compared with Ba_3N and $NaBa_3N$. In many ways, these DOS profiles are similar to those of the alkali metal suboxides which also have narrow anion 2*p* bands and conduction bands formed from metal orbitals [224]. In the subnitrides, the width of the conduction band increases with sodium content, x.

Discrete A_6N units also exist in the '0D' structures of compounds $Na_{16}Ba_6N$ and $Ag_{16}Ca_6N$ [225]. The former compound was first discovered as a minority crystalline phase in bulk Na_2Ba with the ppm levels of nitrogen required for nitriding originating from the dried and deoxygenated argon gas environment under which the alloy preparation was performed. The latter compound was then synthesised by melting together distilled calcium metal and silver shot under argon at 780°C, followed by reaction under nitrogen at 700°C. The two isostructural compounds form body centred cubes with the NA_6 octahedra at the corners and centres of these cubes. Sodium or silver atoms from the surrounding matrix cap faces of two opposing NA_6 octahedra in a trigonal anti-prismatic conformation. From the interatomic distances within and without the discrete octahedra, it is apparent that the bonding regime is ionic and metallic, respectively. As might be expected, four probe resistivity measurements on gold coloured $Ag_{16}Ca_6N$ (which is, perhaps surprisingly, air-stable) confirm metallic behaviour with temperature. It is postulated that the silver subnitride is the correct formulation for the previously reported alloy Ag_8Ca_3 [226] — with the addition of 0.7% nitrogen, the previously empty Ca_6 octahedra in the alloy structure become filled.

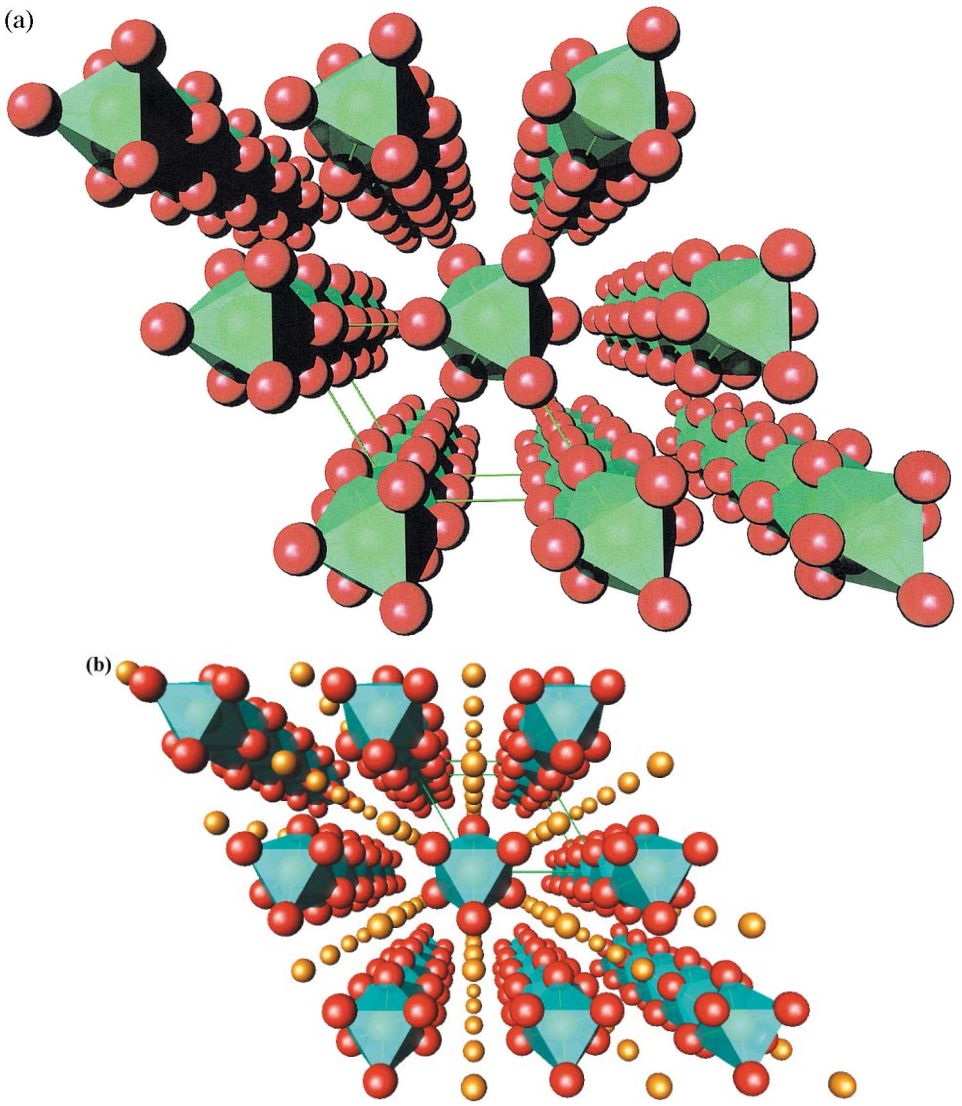

Fig. 12. Structures of the Na_xBa_3N subnitrides ($x = 0$, 1, 5). (a) Ba_3N — chains of face sharing NBa_6 octahedra form parallel columns held together by free electrons alone, whereas (b) $NaBa_3N$ and (c) Na_5Ba_3N contain similar columns in an increasingly vast sodium matrix. Large red spheres depict N, medium orange spheres Na.

Other discrete clusters in subnitrides include the more complex $Ba_{14}Ca(Sr)N_6$ unit which exists within matrices of sodium of varying content within the family $Na_nBa_{14}Ca(Sr)N_6$ ($n = 8$, 14, 17, 21, 22) [227–231]. Crystals of the $n = 14$ member of the family were originally grown in a liquid mixture of NaK alloy (Na:K = 3:1) and barium pre-treated with nitrogen (Ba:N = 3:1). Originally identified as

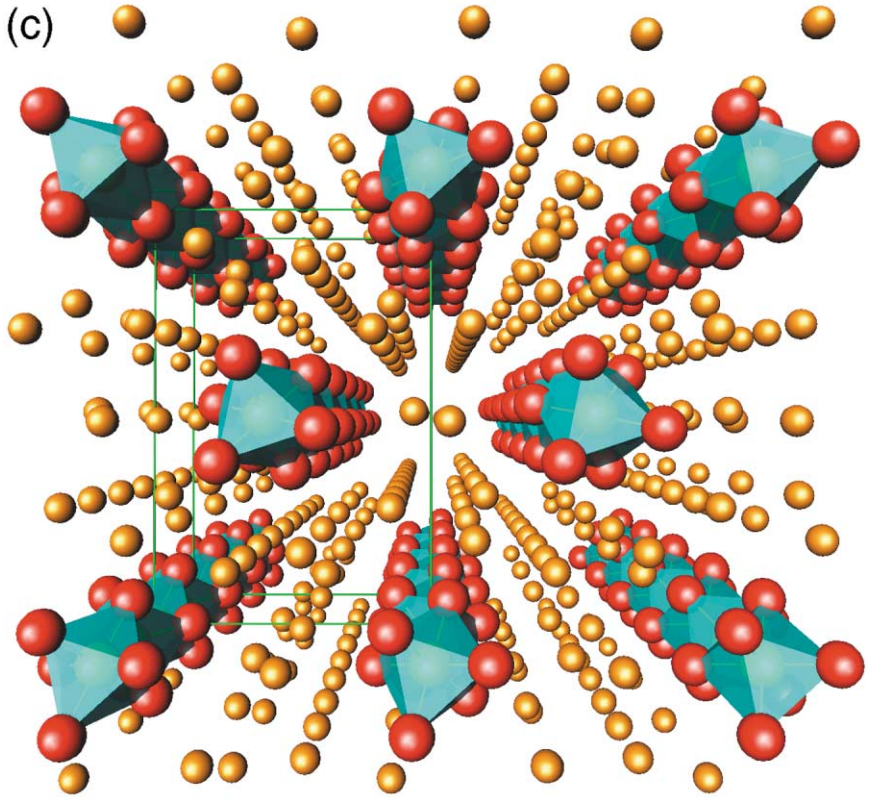

Fig. 12. (*Continued*)

'$Ba_{14}KCaN_6$', the single crystal X-ray structure refinement improved upon 'converting' K atoms to Ca. Subsequently the compound was made as a majority phase by reacting the above reagents with calcium metal [227]. The original source of the calcium was determined to be impurities in the Ba metal. The common unit in this grouping, the $Ba_{14}Ca(Sr)N_6$ cluster, can be considered in several ways, in the first instance it is built around a CaN_6 octahedron which is interpenetrated by a cube of eight barium atoms; the faces of the Ba cube are then capped by a further six Ba atoms. Alternatively, one can view the unit in terms of the familiar subnitride anti-octahedron NA_6 — here six NBa_5Ca octahedra each share four of eight faces, centred at the common Ca vertex (Fig. 13). The packing of the clusters becomes especially complex in the $n = 22$ compound where chains of $Ba_{14}Ca(Sr)N_6$ clusters spaced with Na_6 rings form a hexagonal rod packing with a disorder along the rod direction [228–230]. The rods exhibit a shape periodicity creating two distinct types (A and B) related by a 6_3 screw axis and rendering random packing impossible. This periodicity is probably chiefly geometric, brought about by the alternation of clusters and sodium rings. Orientational disorder, therefore, results from frustration

in the packing as A and B type rods attempt to exclusively neighbour each other heterotypically, with analogies to the anti-ferromagnetic 2-D triangular lattice Ising spin system. The electronic structure of $Na_{22}Ba_{14}SrN_6$ is very similar in most respects to those of the 1-D compounds Na_xBa_3N, notably with a narrow N 2*p* band and a conduction band with no significant N 2*p* character [210].

There are several isolated examples of other subnitrides of varying dimensionality either built up from NA_6 or more complex clusters. These compounds typically incorporate main group (p-block) or late transition metal elements in some way within the alkaline earth subnitride framework. Ca_3AuN like Ca_2AuN is a subnitride auride containing NCa_6 octahedra [232]. Unlike Ca_2AuN and unlike Na_xBa_3N compounds, for example, the octahedra are linked neither in layers nor chains but by corners three dimensionally in an anti-pervoskite structure. Although structurally similar to the main group calcium nitride anti-perovskites Ca_3NX (X = P, As, Sb, Bi, Ge, Sn, Pb) [233], the bonding in the auride is quite different. The Ca_3NX series above can be formulated on the basis of band structure calculations as ionic compounds $(Ca^{2+})_3X^{3-}N^{3-}$ [234,235]. ASW calculations, however, sup-

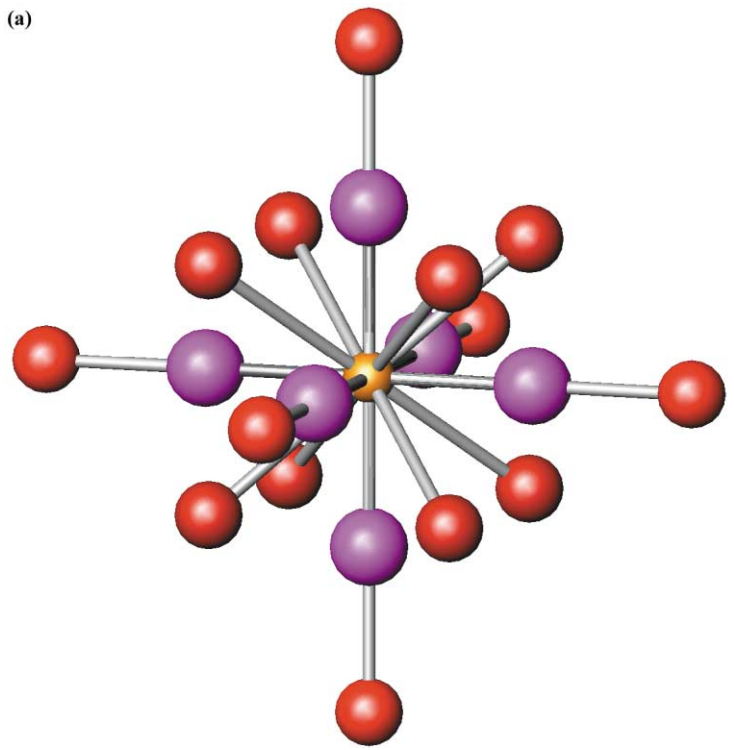

Fig. 13. The discrete $Ba_{14}Ca(Sr)N_6$ cluster found in the $Na_nBa_{14}Ca(Sr)N_6$ ($n = 8$, 14, 17, 21, 22) subnitrides showing (a) bonding of Ba (medium red spheres) in cubic and octahedral environments and N (large violet spheres) in an octahedral environment around the central Ca (Sr) atom and (b) the formation of the cluster via the linking of $NCa(Sr)_6$ octahedra by face-sharing.

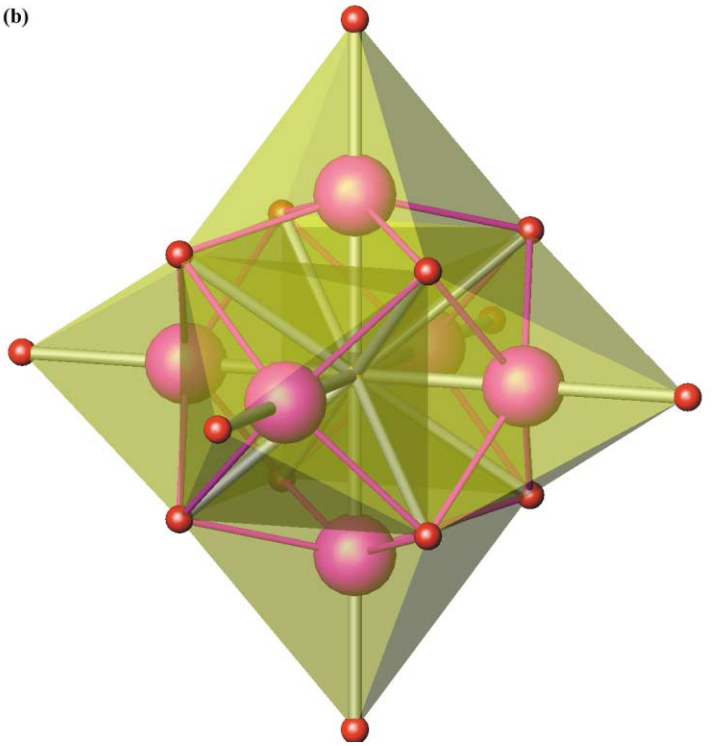

Fig. 13. (*Continued*)

port electronegativity arguments that the auride is a metallic subnitride $(Ca^{2+})_3$-$Au^{-}N^{3-}$ • $(2e^{-})$ with energetically low-lying filled N 2*p* and Au 6*s* and 5*d* bands [232]. (A_6N) $[Ga_5]$ (A = Sr, Ba) contain discrete A_6N octahedra bound together by trigonal bipyramidal $[Ga_5]^{7-}$ polyanions and two free electrons and is thus rationalised as $(A_6N)^{9+}$ $[Ga_5]^{7-}$• $(2e^{-})$ [236]. The bonding in these octahedra is therefore ionic, between A^{2+} and N^{3-}, as in the other subnitrides. The $[Ga_5]^{7-}$ cluster is a homonuclear 22 electron Zintl anion which can be termed a *closo* cluster with $2n + 2 = 12$ electrons in the skeleton according to Wade's rules. The proposed bonding scheme is supported by ASW calculations for A = Sr which describe a metallic band structure with Ga *p* states delocalised over the $[Ga_5]^{7-}$ clusters and only weak overlap between gallium and strontium (barium). Clusters of group 13 metals with similar or lower coordination numbers are observed in other ternary nitrides with an alkaline earth subnitride basis such as CaGaN (square based Ga pyramids joined by edges), $Ca(Sr)_4In_2N$ (zig-zag in chains between $[Ca_4N]^{5-}$ layers of corner-sharing NCa_6 octahedra) and $Ca_5Ga_2N_4$ (zig-zag Ga chains in which each Ga is also coordinated to two terminal nitrogens to form $[Ga(Ga_2N_2)]$ tetrahedra) [237–239].

An example of a compound containing a more complex subnitride cluster within a 'Zintl matrix' is the recently reported $Ag_8Ca_{19}N_7$ [240]. The alkaline earth nitride unit here is the $Ca_{19}N_7$ superoctahedron in which the innermost core of the cluster is a Ca-centred octahedron (CaN_6). Each octahedron is edge capped by a further 12 Ca in a cuboctahedral arrangement. The final 'layer' of the cluster is then completed by six calcium atoms arranged octahedrally around the nitrogen vertices of the central CaN_6 octahedron. The cluster is thus one of six face-sharing NCa_6 octahedra. The superoctahedra are bridged in three dimensions by nitrogen or alternatively the $[N_6(Ca)Ca_{12}]$ unit could be considered linked by NCa_6 octahedra. Each $Ca_{19}N_7$ cluster is then surrounded by eight tetrahedral Ag_4 Zintl-type anions in a primitive cubic arrangement. From structural considerations and extended Huckel calculations, the compound can be formalised as $(Ag_4)_2^{7-}$ $(Ca_{19}N_7)^{17+}\bullet(3e^-)$ with the superoctahedra as ionic entities composed of Ca^{2+} and N^{3-} ions. The band structure of the metallic nitride shows that the DOS around the Fermi level is dominated by the Ag states although some significant contribution of Ca orbitals is also suggested. As with the earlier discussions revolving around the A_2N compounds, there are persuasive arguments for (inadvertent) inclusion of hydrogen into the complex subnitride cluster compounds rather than adopting a formalism incorporating free electrons. As with the layered subnitrides previously, however, the balance of evidence counters such suggestions on grounds of thermodynamics, electronic structure and bonding and observed properties.

4. Ternary nitrides of the s-block metals

Ternary (and higher) compounds composed only of group 1 and 2 metals are relatively few in numbers. Those featuring combinations of group 1 and group 2 metals are principally ionic in nature. Whereas ternary nitrides containing exclusively group 2 metals and nitrogen are sparse and favoured by the lighter elements of the group, it is perhaps not surprising given the incidence of stable alkali metal binary nitrides that no ternary nitrides composed only of group 1 metals and nitrogen are known.

4.1. Group 1/group 2 compounds

Only lithium of the alkali metals forms ternary nitrides with group 2 metals (with alkali metal–nitrogen bonds; i.e. aside from the subnitrides above). This is again unsurprising considering no (meta)stable binary nitrides have been conclusively isolated for sodium through to rubidium. However, it should be noted that bonds between nitrogen and the heavier alkali metals are apparently stable in a small number of ternary nitrides incorporating second and third row transition metals such as those from groups 5 and 6 and p-block elements such as phosphorus [2,241,242].

Lithium beryllium nitride, LiBeN, was first reported by Brice et al. as a result of the reaction between lithium nitride, Li_3N and either Be_3N_2 or beryllium metal in

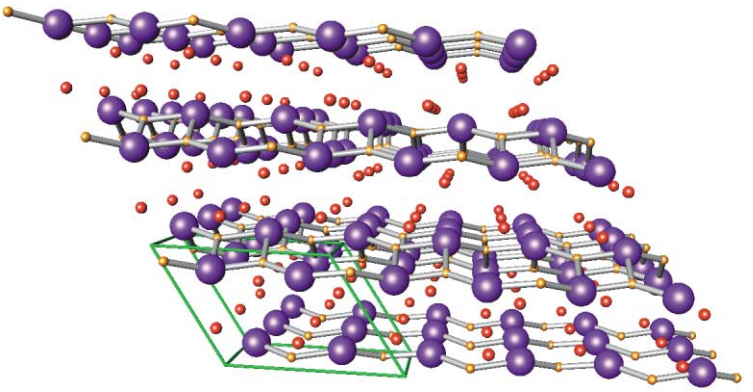

Fig. 14. Structure of LiBeN showing 2-D nets of BeN_3 triangles, $^{2}_{\infty}[BeN_{3/3}]^{-}$, held together by lithium ions (small red circles), small orange spheres represent Be, large blue spheres represent N.

a nitrogen atmosphere at 580°C [243]. The composition of the product was analytically determined and a powder X-ray diffraction pattern was indexed on an orthorhombic unit cell. The ternary nitride was observed to hydrolyse readily, evolving ammonia. Later studies of the ternary system, following a similar preparative strategy, yielded single crystals at higher temperature (1275 K) [244]. The diffraction data for LiBeN was solved, however, in monoclinic space group $P2_1/c$ and gives a structure for the nitride containing corrugated, anionic 2-D layers of composition $^{2}_{\infty}[BeN_{3/3}]^{-}$ similar to those found in EuPdGe (with the EuNiGe structure) [245]. The layers are held together by Li atoms (Fig. 14). Each Be is three-coordinate to N within the anionic layers while Li is surrounded by nitrogen in a distorted tetrahedral geometry. The calculated X-ray powder pattern from the later data is in good agreement with the earlier report suggesting the two compounds have the same identity. Little is known regarding the properties of the nitride.

The only reported compound in the Li–Mg–N system is the 1:1:1 composition LiMgN [246,247]. The ternary nitride is one of a number of compounds originally reported by Juza and co-workers to crystallise with the anti-fluorite structure or related superstructures — these structures are prevalent for lithium ternary nitrides formed with early transition metals, zinc and phosphorus, for example [61]. The ternary nitride is synthesised by the reaction of lithium nitride and magnesium nitride in a nitrogen atmosphere at temperatures of 800–850°C. The resulting product has a simple cubic anti-fluorite structure in which Li and Mg are statistically distributed over the eight equivalent tetrahedral (1/4, 1/4, 1/4) positions. Similarly, only one ternary compound has been reported to date in the Li–Ca–N system. The structure of LiCaN is again different to both LiBeN and LiMgN, although it is closely related to the latter. The compound was originally synthesised from Li_3N with either Ca metal or Ca_3N_2 under nitrogen at 600°C but could not be indexed on the basis of its X-ray powder diffraction pattern [248]. Crystals were later synthesised by the reaction of lithium and calcium metals under nitrogen at

850°C [249]. LiCaN adopts a distorted orthorhombic anti-fluorite structure in which Ca occupies half the tetrahedral holes and Li is displaced from the centres of the remaining half of the metal tetrahedral positions (Fig. 15). Consequently, Li becomes coordinated to N in a trigonal planar geometry similar to that found in Li_3N (although, clearly here the triangle is distorted). Ca is tetrahedrally coordinated to nitrogen, as in α-Ca_3N_2 and nitrogen forms pentagonal bipyramids with Ca (two axial and two equatorial) and Li (three equatorial). The standard enthalpy of formation for LiCaN was determined by drop calorimetry to be -216.8 ± 10.8 kJ mol^{-1} although the enthalpy of formation from the binary nitrides is much smaller (-14.9 ± 11.1 kJ mol^{-1}) [250]. Nickel substitution is possible for lithium in the solid solution, $Ca(Ni_{1-x}Li_x)N$, but only appears to be continuously stable in the nickel rich region of the phase diagram ($0 \leq x \leq 0.58$) [251]. The quaternary nitrides so-formed adopt the YCoC structure of CaNiN [252].

By contrast two compounds are known in the Li–Sr–N system. LiSrN was originally reported in 1970 by Brice et al. as the product of the reaction of 'Sr_3N_2' with either lithium metal or lithium nitride in a nitrogen atmosphere at 600°C or

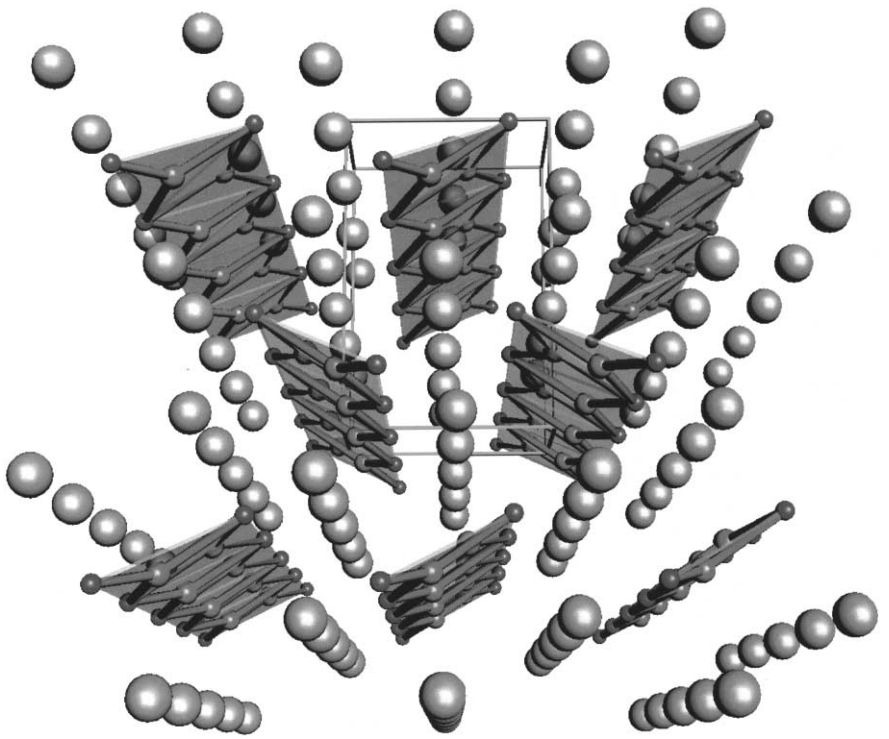

Fig. 15. Structure of LiCaN showing chains of LiN_3 triangles, $^1_\infty[LiN_{3/3}]^{2-}$, running parallel to the [001] direction. The chains of triangles are held together by Ca (medium spheres) in tetrahedral coordination to N (small dark spheres). Lithium atoms are shown as small red spheres at the centre of triangles.

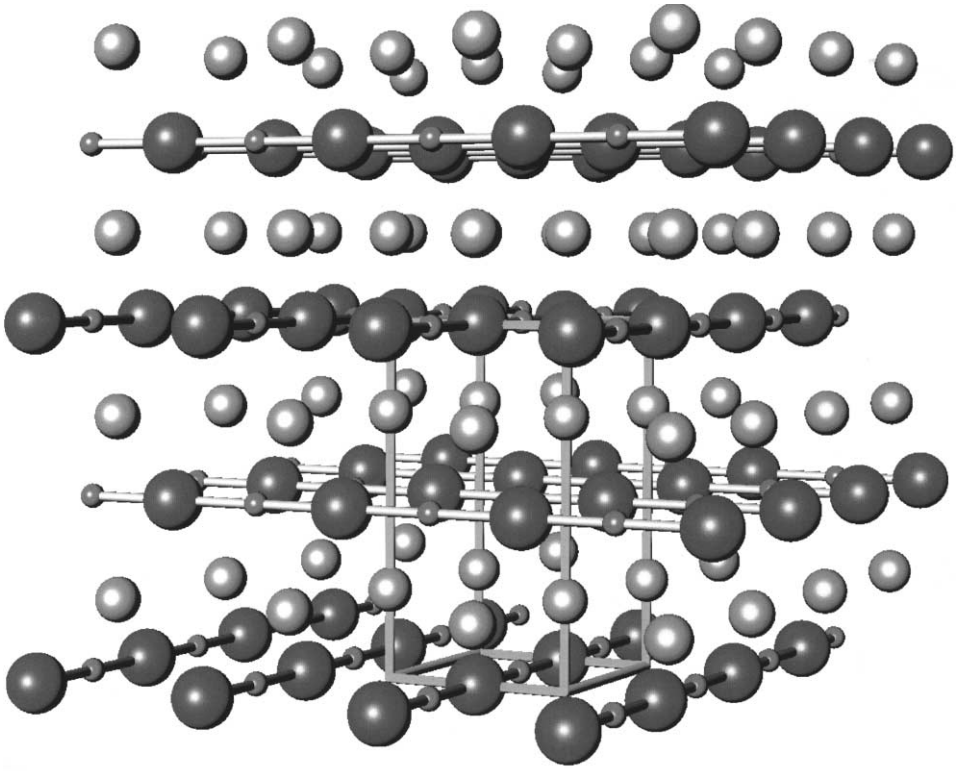

Fig. 16. Structure of LiSrN. Linear, N–Li–N- chains stack along the z direction alternating direction by 90° (parallel to [100], [010] etc.) with each displacement of $c/2$. Lithium atoms are shown as small red spheres, Sr atoms as medium orange spheres and N as large violet spheres.

alternatively as the nitridation product of a pre-heated mixture of lithium and strontium metal (heated under Ar to 750°C) [253]. The composition was determined by analytical techniques and the X-ray powder diffraction pattern of the nitride was indexed on a tetragonal cell ($a = 11.08$ Å, $c = 13.40$ Å). The same authors also noted that a solid solution exists between LiSrN and Li_2O with compounds apparently forming anti-fluorite structures analogous to LiMgN. Subsequent study of the Li–Sr–N system revealed that the 'single' product observed by Brice et al. was a mixture of two phases, LiSrN and Li_4SrN_2 [249,254]. Crystals of LiSrN were obtained by the 1:1 reaction of Li_3N with strontium under nitrogen at 700°C followed by slow cooling over 12 h. The ternary 1:1:1 compound is isostructural with YCoC (and Ca(Li,Ni)N) and contains $[LiN]^{2-}$ chains of Li–N linear units running perpendicular to the c direction which are successively rotated by 90° in the ab plane (i.e. running parallel to [100], [010], [100]… etc.) after translations of 1/2 c (Fig. 16). Strontium is tetrahedrally coordinated to nitrogen whereas nitrogen itself is coordinated in a distorted 'squashed' octahedral geometry to Li (axial) and Sr (equatorial).

The structure of Li_4SrN_2 is very different and more closely resembles Li_3N [249]. The hexagonal bipyramids, NLi_6, in Li_3N are replaced by pentagonal bipyramids, NLi_5Sr_2, in Li_4SrN_2 and the edge-sharing layers in the binary compound are rearranged in the ternary compound such that successive 'double layers' of pentagonal bipyramids are rotated by 90° relative to each other along the [001] direction (Fig. 17). Each 'double layer' is connected through strontium vertices and Sr sits within a distorted tetrahedral geometry to nitrogen. Impedance measurements show that although Li_4SrN_2 is a Li^+ ion conductor, its conductivity is reduced relative to Li_3N. The activation energy for conduction has been measured at 0.9(5) eV although there are no details as yet as to a possible conduction mechanism and no evidence of lithium vacancies. Nickel substitutes for Sr in LiSrN as in LiCaN but again only in the nickel-rich part of the phase diagram ($SrLi_xNi_{1-x}N$; $0 \leq x \leq 0.52$) and the quaternary nitride adopts the SrNiN structure (isostructural with BaNiN) in this region rather than that of LiSrN [255,256]. $Sr(Li_{1-x}Cu_x)N$ forms with the same structure but in a narrower composition range ($0.33 \leq x \leq 0.53$) [257]. Likewise, a copper substituted equivalent of Li_4SrN_2, $Li_{4-x}Cu_xSrN_2$, is observed, for $0 \leq x \leq 0.39$ [257]. Unlike the 1:1:1 compositions, this quaternary phase retains the structure of the parent group 1/group 2 ternary. Another Li–Sr–Ni–N quaternary nitride, $Li_{5-x}Ni_xSr_2N_3$, exists as an intergrowth between $Li_{1-x}Ni_xSrN$ and Li_4SrN_2 for $x = 0.22$ although no evidence for the $x = 0$ non-substituted phase is yet in existence [258].

The chemistry of the Li–Ba–N system is the least well defined of the group 1/group 2 ternary nitride systems. Only LiBaN has been reported in this system [259]. The nitride is prepared either by reaction of the respective binary phases under nitrogen at 600°C or by nitriding a stoichiometric lithium–barium melt at a similar temperature. The black ternary product reacts extremely rapidly with air. LiBaN was indexed on a hexagonal unit cell ($a = 6.79$ Å, $c = 8.05$ Å) from its X-ray powder diffraction pattern. The structure has yet to be solved. As with LiSrN, it is reported that LiBaN forms a solid solution with Li_2O, which can be matched seemingly to a cubic anti-fluorite structure isostructural to LiMgN.

4.2. Group 2 compounds

Ternary nitrides containing exclusively alkaline earth metals are, at present, a rare breed. Current work is beginning to uncover compounds in these ternary systems [146,260]. Early work in the Mg–Ca–N system unearthed a compound of stoichiometry $Mg_3Ca_3N_4$. The violet nitride was prepared from the respective binary nitrides in a nitrogen atmosphere at 800°C, was readily hydrolysed in air and reacted under oxygen at 350°C to give the respective binary oxides. The X-ray powder diffraction pattern was different to that of the two reactants but could not be indexed. $CaMg_2N_2$ has since been synthesised as a bulk powder and as single crystals [146,261]. Both experimental and calculated powder patterns bear a near-identical resemblance to $Mg_3Ca_3N_4$ suggesting the true identity of the earlier nitride is the latter 1:2:2 compound. Powders of $CaMg_2N_2$ were synthesised from 1:2 ratios of the binary nitrides under nitrogen at 1050°C while crystals were grown from

mixtures of Ca, Mg and NaN_3 at 1000 K over approximately 2 days. Both studies produced products with an anti-La_2O_3-type structure with octahedral and tetrahedral coordination of Ca and Mg to nitrogen, respectively. Layers of edge-sharing MgN_4 tetrahedra alternate with layers of edge-sharing CaN_6 octahedra along the z direction in a structure that is also adopted by Li_2ZrN_2, Li_2HfN_2 and Li_2CeN_2 [74–76,262].

Recent studies have also shown that an equivalent compound exists in the Mg–Sr–N system of composition $SrMg_2N_2$ [146]. Single crystals were grown by reaction of Sr and Mg metals with NaN_3 in 1:2:1 ratio in sealed Nb tubes at 1000 K. The transparent colourless plates yielded diffraction data solved as isostructural to $CaMg_2N_2$. The differences in colour between both transparent $CaMg_2N_2$ and $SrMg_2N_2$ and violet '$Ca_3Mg_3N_4$' suggest impurities in the bulk powder product of the originally reported compound. No analogous compound (or any other ternary nitride) was observed in the Mg–Ba–N system.

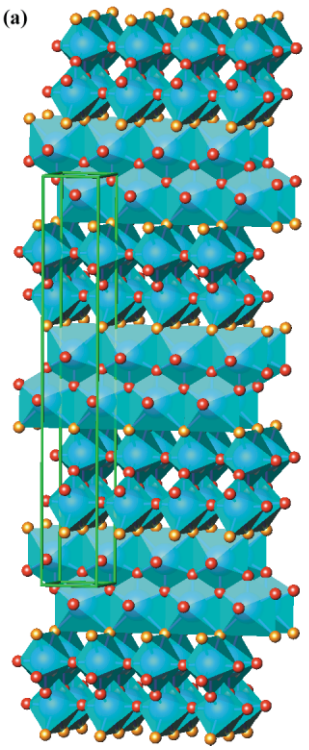

Fig. 17. Structure of Li_4SrN_2. (a) Anion-centred polyhedral representation showing linking of ($NLi_{2/2}Li_{3/3}Sr_{2/4}$) pentagonal bipyramids. Layers of edge-sharing N–(Li,Sr) polyhedra stack along the c-axis. Each slab is two polyhedra 'thick' and is oriented by 90° relative to the previous layer. Each double layer is connected to the next via vertices (Sr atoms); (b) cation-centred polyhedral representation, where $^1_\infty[LiN_{3/3}]^{2-}$ chains stack along the z direction with each section of chains alternating in direction by 90° (parallel to [100], [010] etc.) relative to the next. Chains are linked via SrN_4 tetrahedra.

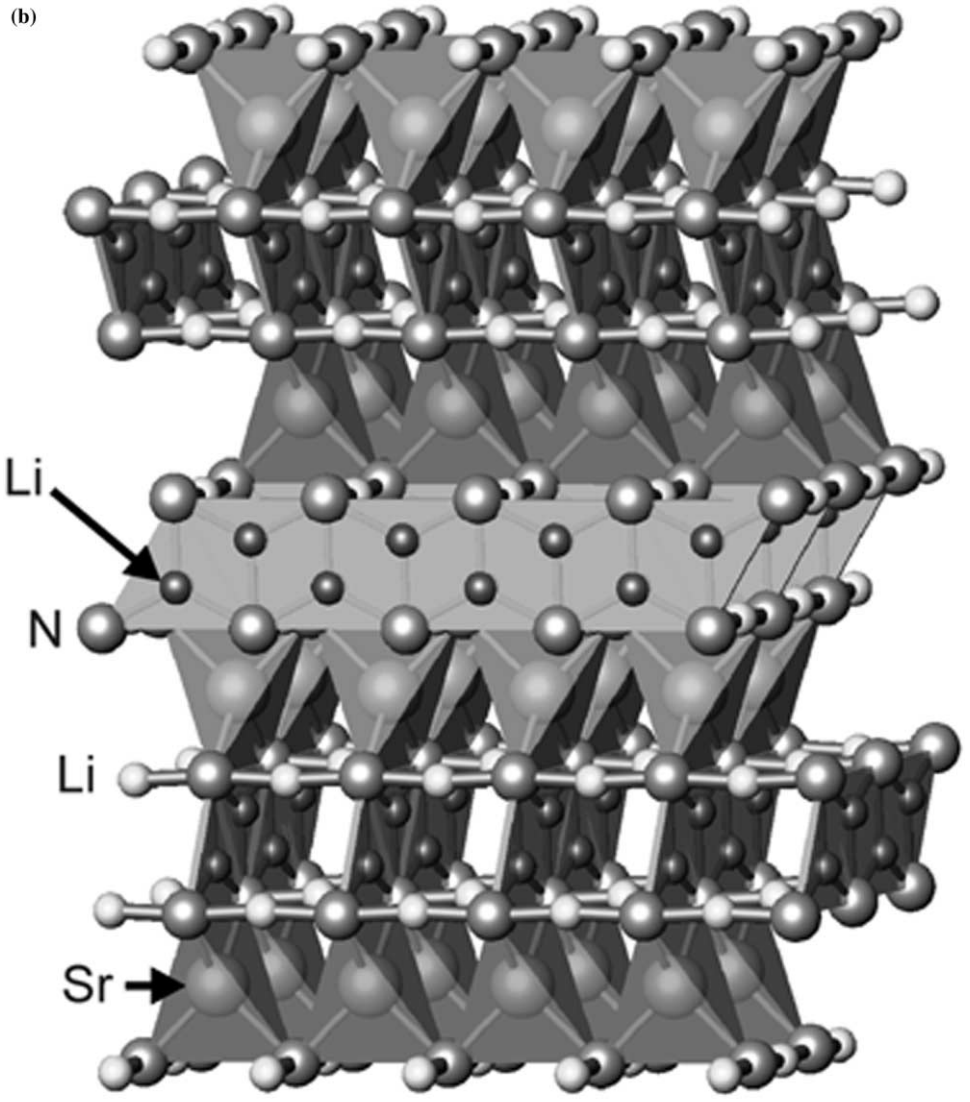

Fig. 17. (*Continued*)

Compounds formed between the heavier alkaline earth metals and nitrogen have yet to be reported in any detail in the literature, although some mention is made of $(Sr_{1-x}Ba_x)_2N$ [210]. Careful synthetic procedures and powder X-ray studies have shown that limited solid solutions exist between the various A_2N subnitride types (A = Ca, Sr, Ba) [260]. Obtaining single phase samples of these ternary subnitrides, however, remains a significant challenge.

5. Concluding remarks

Nitride chemistry is clearly a rapidly evolving area which is now developing sufficiently that distinct fields are defined much as in other areas of solid state and materials chemistry. While traditionally, perhaps, the opportunities afforded by the unique redox chemistry of the transition metals has led to their domination of many branches of inorganic chemistry, it is also apparent that in the solid state chemistry of the nitrides, the frequently neglected s-block metals provoke some interesting and fundamental questions. Indeed, the role of these electropositive elements in stabilising otherwise unattainable bonding environments cannot be overemphasised. Yet, from binary through to quaternary and higher combinations of the s-block elements alone, the solid state chemist witnesses the whole gamut of chemical bonding from the most ionic through degrees of covalency to compounds approaching the metallic regime. These often unique amalgamations of bonding within solids lead to highly unusual crystal and coordination chemistry. Our synthetic exploration of the group 1 and 2 nitrides is clearly far from over. Moreover, our investigations of the properties of these materials is at a very early level. Just as our understanding of the structure-property relations in the s-block nitrides inevitably improves, we are also likely to be frequently surprised.

Acknowledgements

The author would like to thank warmly Dr R.J. Pulham, Dr P. Hubberstey and Dr M.G. Barker for many useful discussions while compiling this work and also Dr N.E. Brese and Dr O. Reckeweg for illuminating conversations and pre-prints of manuscripts. The author would also like to acknowledge the EPSRC for the award of an Advanced Research Fellowship and for funding relevant research projects.

References

[1] D.H. Gregory, J. Chem. Soc. Dalton Trans. (1999) 259.
[2] R. Niewa, F.J. DiSalvo, Mater. Chem. 10 (1998) 2733.
[3] J. Etourneau, J. Portier, F. Monil, J. Alloys Compd. 188 (1992) 1.
[4] W. Schnick, Angew. Chem. Int. Ed. Engl. 32 (1993) 806.
[5] W. Schnick, Comments Inorg. Chem. 17 (1995) 189.
[6] W. Schnick, H. Huppertz, Chem. Eur. J. 3 (1997) 679.
[7] S.J. Clarke, G.R. Kowach, F.J. DiSalvo, Inorg. Chem. 35 (1996) 7009.
[8] H. Yamane, F.J. DiSalvo, J. Alloys Compd. 241 (1996) 69.
[9] S.J. Clarke, F.J. DiSalvo, J. Alloys Compd. 259 (1997) 158.
[10] A. Simon, Coord. Chem. Rev. 163 (1997) 253.
[11] C. Röhr, Angew. Chem. Int. Ed. Engl. 35 (1996) 1199.
[12] N.A. Brese, M. O'Keeffe, Struct. Bonding (Berlin) 79 (1982) 307.
[13] L. Ouvrard, C. R. Acad. Sci. Paris 114 (1892) 120.
[14] R. Brill, Z. Kristallogr. 65 (1927) 94.
[15] E. Zintl, G. Brauer, Z. Elektrochem. 41 (1935) 102.

[16] F. Gallais, E. Masdupuy, C. R. Acad. Sci. Paris C227 (1948) 635.
[17] U.v. Alpen, J. Solid State Chem. 29 (1979) 379.
[18] A. Rabenau, Solid State Ionics 6 (1982) 277.
[19] C.C. Addison, B.M. Davis, J. Chem. Soc. (A) (1969) 1827.
[20] M.G. Down, P. Hubberstey, R.J. Pulham, J. Chem. Soc. Dalton Trans. (1975) 1490.
[21] C.C. Addison, The Chemistry of the Liquid Alkali Metals, Wiley, New York, 1984.
[22] R.J. Pulham, P. Hubberstey, A.E. Thunder, A. Harper, A.T. Dadd, in: Proceedings of the Second International Conference on Liquid Metal Technology in Energy Production, Richland, April 1980.
[23] P.F. Adams, P. Hubbertsey, R.J. Pulham, J. Less-Common Met. 42 (1975) 1.
[24] E. Schönherr, G. Müller, E. Winkler, J. Crystallogr. Growth 43 (1978) 469.
[25] D.W. Osborne, H.E. Flotow, J. Chem. Thermodyn. 10 (1978) 675.
[26] J. Barin, O. Knacke, O. Kubaschewski, Thermodynamical Properties of Inorganic Substances, Springer, Berlin/New York, 1977.
[27] A. Rabenau, H. Schulz, J. Less-Common Met. 50 (1976) 155.
[28] B.A. Boukamp, R.A. Huggins, Mater. Res. Bull. 13 (1978) 23.
[29] H. Schulz, K. Schwarz, Acta Crystallogr. Sect. A 34 (1978) 999.
[30] H.R. Chandrasekhar, G. Bhattacharya, R. Migoni, H. Bilz, Phys. Rev. B 17 (1978) 884.
[31] W. Kress, H. Grimm, W. Press, J. Lefebvre, Phys. Rev. B 22 (1980) 4620.
[32] P. Pattison, J.R. Schneider, Acta Crystallogr. Sect. A 36 (1980) 390.
[33] P. Pattison, N.K. Hansen, J.R. Schneider, Acta Crystallogr. Sect. B 40 (1984) 38.
[34] O. Aikala, Acta Crystallogr. Sect. A 40 (1984) C169.
[35] G. Kerker, Phys. Rev. B 23 (1981) 6312.
[36] H. Brendecke, W. Bludau, J. Appl. Phys. 50 (1979) 4743.
[37] R. Dovesi, C. Pisani, F. Ricca, C. Roetti, V.R. Saunders, Phys. Rev. B 30 (1984) 972.
[38] M. Causá, R. Dovesi, C. Pisani, C. Roetti, Phys. Rev. B 32 (1985) 1196.
[39] P.W. Fowler, P. Tole, R.W. Munn, M. Hurst, Mol. Phys. 67 (1989) 141.
[40] H. Schulz, K.H. Thiemann, Acta Crystallogr. Sect. A 35 (1979) 309.
[41] U.H. Zucker, H. Schulz, Acta Crystallogr. 568 (1982) 568.
[42] J. Wahl, Solid State Commun. 29 (1979) 485.
[43] A. Hooper, T. Laap, S. Skaarup, Mater. Res. Bull. 14 (1979) 1617.
[44] M.F. Bell, A. Breitschwerdt, U.v. Alpen, Mater. Res. Bull. 16 (1981) 267.
[45] J.O. Thomas, R. Tellgren, Solid State Ionics 5 (1981) 407.
[46] U.v. Alpen, A. Rabenau, G.H. Talat, Appl. Phys. Lett. 30 (1977) 621.
[47] S.G. Bishop, P.J. Ring, P.J. Bray, J. Chem. Phys. 45 (1966) 1525.
[48] P.K. Burkert, H.P. Fritz, G. Stefaniak, Z. Naturforsch. 25b (1970) 1220.
[49] D. Brinkmann, W. Freudenreich, J. Roos, Solid State Commun. 28 (1978) 233.
[50] K. Differt, R. Messer, J. Phys. C 13 (1980) 717.
[51] J. Lewis, D. Schwarzenbach, Acta Crystallogr. Sect. A 37 (1981) 507.
[52] P. Blaha, K. Schwarz, P. Herzig, Phys. Rev. Lett. 54 (1985) 1192.
[53] R. Messer, H. Birli, K. Differt, J. Phys. C 14 (1981) 2731.
[54] E. Bertold-Schweickert, M. Mali, J. Roos, D. Brinkmann, Phys. Rev. B 30 (1984) 2891.
[55] B. Bader, P. Heitjans, H.J. Stöckmann, W. Buttler, P. Freiländer, G. Kiese, C. van der Marel, A. Schirmer, J. Phys. Condens. Matter 4 (1992) 4779.
[56] M.L. Wolf, J. Phys. C 17 (1984) L285.
[57] M.L. Wolf, J.R. Walker, C.R.A. Catlow, J. Phys. C 17 (1984) 6623.
[58] M.L. Wolf, C.R.A. Catlow, J. Phys. C 17 (1984) 6635.
[59] S. Ihara, K. Suzuki, Phys. Lett. 110A (1985) 265.
[60] J. Sarnthein, K. Schwarz, P.E. Blöchl, Phys. Rev. B 53 (1996) 9084.
[61] R. Juza, K. Langer, K.v. Benda, Angew. Chem. Int. Ed. 7 (1968) 360.
[62] A. Gudat, S. Haag, R. Kniep, A. Rabenau, Z. Naturforsch. 45b (1990) 111.
[63] A. Gudat, R. Kniep, A. Rabenau, Angew. Chem. Int. Ed. Engl. 30 (1991) 199.
[64] J. Klatyk, P. Höhn, R. Kniep, Z. Kristallogr. 213 (1998) 31.
[65] M.G. Barker, A.J. Blake, P.P. Edwards, D.H. Gregory, T.A. Hamor, D.J. Siddons, S.E. Smith, J. Chem. Soc. Chem. Commun. (1999) 1187.

[66] M.T. Weller, S.E. Dann, P.F. Henry, D.B. Currie, J. Mater. Chem. 9 (1999) 283.
[67] D.H. Gregory, P.M. O'Meara, A.G. Gordon, D.J. Siddons, A.J. Blake, M.G. Barker, T.A. Hamor, P.P. Edwards, J. Alloys Compd., in press.
[68] A. Gudat, R. Kniep, A. Rabenau, W. Bronger, U. Ruschewitz, J. Less-Common Met. 161 (1990) 31.
[69] R. Juza, F. Hund, Naturwiss 38 (1946) 121.
[70] R. Juza, F. Hund, Z. Anorg. Allg. Chem. 257 (1948) 1.
[71] R. Niewa, F.J. DiSalvo, D.K. Yang, D.B. Zax, H. Luo, W.B. Yelon, J. Alloys Compd. 266 (1998) 32.
[72] D.A. Vennos, F.J. DiSalvo, Acta Crystallogr. Sect. C 48 (1992) 610.
[73] C. Wachsmann, H. Jacobs, J. Alloys Compd. 190 (1992) 113.
[74] A.P. Palisaar, R. Juza, Z. Anorg. Allg. Chem. 384 (1971) 1.
[75] M.G. Barker, I.C. Alexander, J. Chem. Soc. Dalton Trans. (1974) 2166.
[76] R. Niewa, H. Jacobs, H.M. Mayer, Z. Kristallogr. 210 (1995) 513.
[77] N. Nishijima, Y. Takeda, N. Ishmanishi, O. Yamamoto, J. Solid State Chem. 113 (1994).
[78] S. Suzuki, T. Shodai, Solid State Ionics 116 (1999) 1.
[79] T. Asai, K. Nishida, S. Kawai, Mater. Res. Bull. 19 (1984) 1377.
[80] T. Shodai, S. Okada, S. Tobishima, J. Yamaki, J. Power Sources 68 (1997) 515.
[81] Y. Takeda, M. Nishijima, M. Yamahata, K. Takeda, N. Imanishi, O. Yamamoto, Solid State Ionics 130 (2000) 61.
[82] W. Schnick, J. Lücke, J. Solid State Chem. 87 (1990) 101.
[83] W. Schnick, J. Lücke, Z. Anorg. Allg. Chem. 588 (1990) 19.
[84] J. David, Y. Laurent, J.P. Carlot, J. Lang, Bull. Soc. Fr. Miner. Cristallogr. 96 (1973) 21.
[85] M. Orth, W. Schnick, Z. Anorg. Allg. Chem. 625 (1999) 1426.
[86] J. David, J. Charlot, J. Lang, Rev. Chim. Minér. 11 (1974) 405.
[87] H. Yamane, S. Kikkawa, H. Horiuchi, M. Koizumi, J. Solid State Chem. 65 (1986) 6.
[88] H. Yamane, S. Kikkawa, M. Koizumi, J. Solid State Chem. 71 (1987) 1.
[89] R. Marx, J. Solid State Chem. 128 (1997) 241.
[90] R. Marx, H.M. Mayer, J. Solid State Chem. 130 (1997) 90.
[91] R. Marx, H.M. Mayer, Z. Naturforsch. 50b (1995) 1353.
[92] R. Marx, H.M. Mayer, Z. Naturforsch. 51b (1996) 525.
[93] R. Marx, Eur. J. Solid State Inorg. Chem. 35 (1998) 197.
[94] R. Marx, Z. Naturforsch. 50b (1995) 1061.
[95] R. Marx, Z. Anorg. Allg. Chem. 623 (1997) 1912.
[96] J.C. Fitzmaurice, A.L. Hector, I.P. Parkin, J. Chem. Soc. Dalton Trans. (1993) 2435.
[97] J.C. Fitzmaurice, A.L. Hector, A.T. Rowley, I.P. Parkin, Polyhedron 13 (1994) 235.
[98] M. Mali, J. Roos, D. Binkmann, Phys. Rev. B 36 (1987) 3888.
[99] H.J. Beister, S. Haag, R. Kniep, K. Strössner, K. Syassen, Angew. Chem. Int. Ed. Engl. 27 (1988) 1101.
[100] S.V. Mitrokhina, K.P. Burdina, K.N. Semenenko, Vestn. Mosk. Univ. Seriya 2 Khimiya 31 (1990) 612.
[101] D.E. Sands, D.H. Wood, W.J. Ramsey, Acta Crystallogr. 16 (1963) 316.
[102] E. Zintl, G. Brauer, Z. Elektrochem. Angew. Phys. Chem. 41 (1935) 297.
[103] A.C. Ho, M.K. Granger, A.L. Ruoff, P.E. Van Camp, V.E. Van Doren, Phys. Rev. B 59 (1999) 6083.
[104] G.J. Moody, J.D.R. Thomas, J. Chem. Educ. 43 (1966) 205.
[105] E. Veleckis, K.E. Anderson, F.A. Cafasso, H.M. Feder, in: Proceedings of the International Conference on Sodium Technology and Large Fast Reactor Design, Report ANL-7520, Part I, 1968, p. 295.
[106] P.F. Adams, M.G. Down, P. Hubberstey, R.J. Pulham, J. Less-Common Met. 42 (1975) 325.
[107] R.J. Pulham, P. Hubberstey, J. Nucl. Mater. 115 (1983) 239.
[108] E.W. Guernsey, M.S. Sherman, J. Am. Chem. Soc. 47 (1925) 1933.
[109] F. Fischer, F. Schröter, Ber. D Chem. Gesellschaft 43 (1910) 1465.
[110] H. Wattenberg, Ber. D Chem. Gesellschaft 63 (1930) 1667.

[111] W. Moldenhauer, H. Möttig, Ber. D Chem. Gesellschaft 62 (1929) 1954.
[112] H. Moissan, Compte. Rend. 136 (1903) 587.
[113] M. Jansen, J.C. Schön, Z. Anorg. Allg. Chem. 624 (1998) 533.
[114] P. Eckerlin, A. Rabenau, Z. Anorg. Allg. Chem. 304 (1964) 218.
[115] C.L. Hoenig, A.W. Searcy, J. Am. Ceram. Soc. 50 (1967) 460.
[116] M.v. Stackelberg, R. Paulus, Z. Phys. Chem. B22 (1933) 305.
[117] R. Juza, H. Jacobs, H. Gerke, Ber. Bunsenges. Physik. Chem. 70 (1966) 1103.
[118] P.I. Taratunin, N.A. Sobol'eva, USSR Patent 1976.
[119] A. Reyes-Serrato, G. Soto, A. Gamietea, M.H. Farías, J. Phys. Chem. Solids 59 (1998) 743.
[120] D.W. Mitchell, Ind. Engng. Chem. Analyt. Edn. 41 (1949) 2027.
[121] J.R. Soulen, P. Sthapitanonda, J.L. Margrave, J. Phys. Chem. 59 (1955) 132.
[122] D.R. Glasson, S.A.A. Jayaweera, J. Appl. Chem. 18 (1968) 77.
[123] H. Mathewson, Z. Anorg. Chem. 48 (1906) 191.
[124] M.G. Barker, unpublished results.
[125] R.S. Bradley, D.C. Munro, M. Whitfield, Z. Anorg. Nucl. Chem. 28 (1966) 1803.
[126] S. Cui, S. Liao, Y. Zhang, Y. Xu, Y. Miao, M. Lu, Y. Fan, W. Guo, J. Mater. Sci. 34 (1999) 5601.
[127] T. Murata, K. Itatani, F.S. Howell, A. Kishioka, M. Kinoshita, J. Am. Ceram. Soc. 76 (1993) 2909.
[128] J. David, Y. Laurent, J. Lang, Bull. Soc. Franc. Min. Crist. 72 (1977) 1949.
[129] D.E. Partin, D.J. Williams, M. O'Keeffe, J. Solid State Chem. 132 (1997) 56.
[130] A.M. Heyns, L.C. Prinsloo, K.-J. Range, M. Stassen, J. Solid State Chem. 137 (1998) 33.
[131] C.M. Fang, R.A. de Groot, R.J. Bruls, H.T. Hintzen, G. de With, J. Phys. Condens. Matter 11 (1999) 4833.
[132] I.S. Gladkaya, G.N. Kremkova, N.A. Bendeliani, J. Mater. Sci. Lett. 12 (1993) 1547.
[133] P. Eckerlin, A. Rabenau, H. Nortmann, Z. Anorg. Allg. Chem. 353 (1967) 113.
[134] P. Eckerlin, Z. Anorg. Allg. Chem. 353 (1967) 225.
[135] J. David, Y. Laurent, J. Lang, Bull. Soc. Fr. Minér. Cristallogr. 35B (1980) 604.
[136] R.J. Bruls, H.T. Hintzen, R. Metselaar, C.K. Loong, J. Phys. Chem. Solids 61 (2000) 1285.
[137] R. Marchand, Y. Laurent, Mater. Res. Bull. 17 (1982) 399.
[138] V. Schultz-Coulon, W. Schnick, Z. Anorg. Allg. Chem. 623 (1997) 69.
[139] P. Verdier, R. Marchand, J. Lang, C. R. Acad. Sci. Paris 271 (1970) 1002.
[140] H.H. Emons, W. Grothe, H.H. Seyfarth, Z. Anorg. Allg. Chem. 363 (1968) 191.
[141] S. Andersson, J. Solid State Chem. 1 (1970) 306.
[142] H. Lorenz, U. Kühne, C. Hohlfield, K. Flegel, J. Mater. Sci. Lett. 7 (1988) 23.
[143] D.H. Gregory, M.G. Barker, P.P. Edwards, D.J. Siddons, Inorg. Chem. 34 (1995) 5195.
[144] Y. Laurent, J. Lang, M.T. LeBihan, Acta Crystallogr. B24 (1968) 494.
[145] P. Höhn, Dissertation, Technische Hochschule, Darmstadt, Germany, 1993.
[146] O. Reckeweg, F.J. DiSalvo, Z. Anorg. Allg. Chem. 627 (2001) accepted for publication.
[147] D.H. Gregory, A. Bowman, C.F. Baker, in preparation.
[148] S.F. Pal'guev, R.P. Lesunova, L.S. Karenina, Solid State Ionics 20 (1986) 255.
[149] P.P. Lesunova, L.S. Karenina, S.F. Pal'guev, E.I. Burmakin, Solid State Ionics 36 (1989) 275.
[150] R.P. Lesunova, S.F. Pal'guev, E.I. Burmakin, Inorg. Mater. 34 (1998) 987.
[151] Y. Laurent, J. David, J. Lang, C. R. Acad. Sci. Paris 259 (1964) 1132.
[152] O. Reckeweg, F.J. DiSalvo, Angew. Chem. Int. Ed. Engl. 39 (2000) 412.
[153] H.H. Franck, M.A. Bredig, G. Hoffmann, Naturwiss 21 (1933) 330.
[154] H. Hartmann, H.J. Fröhlich, Z. Anorg. Allg. Chem. 218 (1934) 190.
[155] J. Aubry, R. Streiff, C. R. Acad. Sci. Paris 263 (1966) 931.
[156] Y. Laurent, J. Lang, M.T. Le Bihan, Acta Crystallogr. B25 (1969) 199.
[157] A. Bowman, C.F. Baker, D.H. Gregory, in preparation.
[158] H. Hartmann, H.J. Fröhlich, F. Ebert, Z. Anorg. Allg. Chem. 218 (1934) 181.
[159] Y. Okamoto, J.C. Goswami, Inorg. Chem. 5 (1966) 1281.
[160] K.H. Linke, H. Lingmann, Z. Anorg. Allg. Chem. 366 (1969) 82.
[161] K.H. Linke, H. Lingmann, Z. Anorg. Allg. Chem. 366 (1969) 89.

[162] K.H. Linke, R. Taubert, T. Kruck, Z. Anorg. Allg. Chem. 396 (1973) 1.
[163] W. Schnick, V. Schultz-Coulon, Angew. Chem. Int. Ed. Engl. 32 (1993) 280.
[164] T. Schlieper, W. Schnick, Z. Anorg. Allg. Chem. 621 (1995) 1037.
[165] V. Schultz-Coulon, W. Schnick, Z. Znorg. Allg. Chem. 623 (1997) 69.
[166] H. Yamane, F.J. DiSalvo, Acta Crystallogr. C52 (1996) 760.
[167] S.J. Clarke, F.J. DiSalvo, Inorg. Chem. 39 (2000) 2631.
[168] J.F. Brice, J.P. Motte, A. Courtois, J. Protas, J. Aubry, J. Solid State Chem. 17 (1976) 135.
[169] P. Ehrlich, W. Linz, H.J. Seifert, Naturwiss 58 (1971) 219.
[170] T. Sichla, H. Jacobs, Eur. J. Solid State Inorg. Chem. 32 (1995) 49.
[171] A. Bowman, C.F. Baker, P.V. Mason, D.H. Gregory, in preparation.
[172] H.H. Emons, D. Anders, G. Roewer, F. Vogt, Z. Anorg. Allg. Chem. 333 (1964) 99.
[173] C. Hadenfeldt, H. Herdejürgen, Z. Anorg. Allg. Chem. 545 (1987) 177.
[174] C. Hadenfeldt, H. Herdejürgen, Z. Anorg. Allg. Chem. 558 (1988) 35.
[175] A. Bowman, C.F. Baker, D.H. Gregory, in preparation.
[176] G. Bocquillon, C. Loriers-Susse, J. Loriers, C. R. Acad. Sci. Paris 315 (Série II) (1992) 1069.
[177] A. Guntz, F. Benoit, Ann. Chim. 20 (1923) 5.
[178] A.v. Antropoff, K.H. Krüger, Z. Phys. Chem. A167 (1933) 49.
[179] J. Gaudé, J. Lang, C. R. Acad. Sci. Paris C271 (1970) 510.
[180] J. Gaudé, J. Lang, Rev. Chim. Minér. 7 (1970) 1059.
[181] J. Gaudé, P. L'Haridon, Y. Laurent, J. Lang, Bull. Soc. Fr. Minér. Crist. 95 (1972) 56.
[182] J. Gaudé, J. Lang, Rev. Chim. Minér. 9 (1972) 799.
[183] J.F. Motte, J.P. Brice, J. Aubry, C. R. Acad. Sci. Paris C274 (1972) 1814.
[184] J.F. Brice, J.P. Motte, J. Aubry, Rev. Chim. Minér. 12 (1975) 105.
[185] N.E. Brese, M. O'Keeffe, R.B. von Dreele, J. Solid State Chem. 88 (1990) 571.
[186] T. Sichla, F. Altorfer, D. Hohlwein, K. Reimann, M. Steube, J. Wrzesinski, H. Jacobs, Z. Anorg. Allg. Chem. 623 (1997) 414.
[187] V. Schultz-Coulon, E. Irran, B. Putz, W. Schnick, Z. Anorg. Allg. Chem. 625 (1999) 1086.
[188] K. Torkar, H.T. Spath, Monatash. Chem. 98 (1967) 2020.
[189] J. Gaudé, J. Lang, C. R. Acad. Sci. Paris C274 (1972) 521.
[190] H.T. Künzel, Thesis, Stuttgart, Germany 1980.
[191] K.H. Linke, K. Schrödter, Z. Anorg. Allg. Chem. 418 (1975) 165.
[192] B. Wegner, R. Essmann, H. Jacobs, P. Fischer, J. Less-Common Met. 167 (1990) 81.
[193] S.M. Ariya, E.A. Prokofyeva, J. Gen. Chem. Suppl. I (1953) 78.
[194] C.C. Addison, G.K. Creffield, P. Hubberstey, R.J. Pulham, J. Chem. Soc. A (1971) 1393.
[195] C.C. Addison, G.K. Creffield, P. Hubberstey, R.J. Pulham, J. Chem. Soc. A (1971) 2688.
[196] P. Hubberstey, in: Proceedings of the Conference on Liquid Alkali Metals, British Nuclear Society, 1973, p. 15.
[197] C.C. Addison, R.J. Pulham, E.A. Trevillion, J. Chem. Soc. Dalton Trans. (1975) 2082.
[198] C.C. Addison, G.K. Creffield, P. Hubberstey, R.J. Pulham, J. Chem. Soc.Dalton Trans. (1976) 1105.
[199] P.R. Bussey, P. Hubberstey, R.J. Pulham, J. Chem. Soc. Dalton Trans. (1976) 1976.
[200] P. Hubberstey, P.R. Bussey, J. Less-Common Met. 60 (1978) 109.
[201] S.M. Ariya, E.A. Prokofyeva, I.I. Matveeva, J. Gen. Chem. USSR 25 (1955) 609.
[202] I. Ahmad, Ph.D. thesis, London, 1963.
[203] E.T. Keve, A.C. Skapski, Chem. Commun. (1966) 829.
[204] E.T. Keve, A.C. Skapski, Inorg. Chem. 7 (1968) 1757.
[205] D.H. Gregory, A. Bowman, C.F. Baker, D.P. Weston, J. Mater. Chem. 10 (2000) 1635.
[206] N.E. Brese, M. O' Keeffe, J. Solid State Chem. 87 (1990) 134.
[207] O. Seeger, Thesis, Tübingen, Germany, 1994.
[208] K. Andres, N.A. Kuebler, M.B. Robin, J. Phys. Chem. Solids 27 (1966) 1747.
[209] N. Hamada, S. Ido, K. Kitazawa, S. Tanaka, J. Phys. C: Solid State Phys. 19 (1986) 1355.
[210] U. Steinbrenner, P. Adler, W. Hölle, A. Simon, J. Phys. Chem. Solids 59 (1998) 1527.
[211] C.M. Fang, G.A. de Wijs, R.A. de Groot, H.T. Hintzen, G. de With, Chem. Mater. 12 (2000) 1847.

[212] H. Smolinski, W. Weber, J. Phys. Chem. Solids 59 (1998) 915.
[213] H. Emons, D. Anders, G. Roewer, F. Vogt, Z. Anorg. Allg. Chem. 333 (1964) 99.
[214] P.F. Henry, M.T. Weller, Angew. Chem. Int. Ed. 37 (1998) 2855.
[215] G. Cordier, P. Höhn, R. Kniep, A. Rabenau, Z. Anorg Allg. Chem. 591 (1990) 58.
[216] D.H. Gregory, M.G. Barker, P.P. Edwards, D.J. Siddons, Inorg. Chem. 34 (1995) 5195.
[217] A. Simon, Z. Anorg. Allg. Chem. 395 (1973) 301.
[218] A. Simon, Angew. Chem. Int. Ed. Engl. 27 (1988) 159.
[219] P.E. Rauch, A. Simon, Angew. Chem. 104 (1992) 1505.
[220] P.E. Rauch, A. Simon, Angew. Chem. Int. Ed. 31 (1992) 1519.
[221] G.J. Snyder, A. Simon, J. Am. Chem. Soc. 127 (1995) 1996.
[222] U. Steinbrenner, A. Simon, Z. Anorg. Allg. Chem. 624 (1998) 228.
[223] K.R. Tsai, P.M. Harris, E.N. Lassettre, J. Phys. Chem. 60 (1956) 345.
[224] G. Ebbinghaus, A. Simon, J. Chem. Phys. 43 (1979) 117.
[225] G.J. Snyder, A. Simon, Angew. Chem. Int. Ed. Engl. 33 (1994) 689.
[226] L.D. Calvert, C. Rand, Acta Crystallogr. 17 (1964) 1175.
[227] U. Steinbrenner, A. Simon, Angew. Chem. Int. Ed. Engl. 35 (1996) 552.
[228] A. Simon, U. Steinbrenner, J. Chem. Soc. Faraday Trans. 92 (1996) 2117.
[229] U. Steinbrenner, A. Simon, Z. Kristallogr. 212 (1997) 428.
[230] U. Steinbrenner, A. Simon, Z. Kristallogr. 212 (1997) 688.
[231] G.V. Vajenine, U. Steinbrenner, A. Simon, C. R. Acad. Sci. Ser. IIc: Chim. 2 (1999) 583.
[232] J. Jäger, D. Stahl, P.C. Schmidt, R. Kniep, Angew. Chem. Int. Ed. Engl. 32 (1993) 709.
[233] M.Y. Chern, D.A. Vennos, F.J. DiSalvo, J. Solid State Chem. 96 (1992) 415.
[234] D.A. Papaconstantopoulos, W.E. Pickett, Phys. Rev. B 45 (1992) 4008.
[235] P.R. Vansant, P.E. Van Camp, V.E. Van Doren, J.L. Martins, Phys. Rev. B 57 (1998) 7615.
[236] G. Cordier, M. Ludwig, D. Stahl, P.C. Schmidt, R. Kniep, Angew. Chem. Int. Ed. Engl. 34 (1995) 1761.
[237] P. Verdier, P. L'Haridon, M. Maunaye, R. Marchand, Acta Crystallogr. Sect. B 30 (1974) 226.
[238] G. Cordier, S. Ronninger, Z. Naturforsch. 42b (1987) 825.
[239] G. Cordier, Z. Naturforsch. 43b (1988) 1253.
[240] O. Reckeweg, T.P. Braun, F.J. DiSalvo, H.J. Meyer, Z. Anorg. Allg. Chem. 626 (2000) 62.
[241] R. Niewa, H. Jacobs, Chem. Rev. 96 (1996) 2053.
[242] K. Landskron, E. Irran, W. Schnick, Chem. Eur. J. 5 (1999) 2548.
[243] J.F. Brice, J.P. Motte, R. Streiff, C. R. Acad. Sci. Paris C269 (1969) 910.
[244] M. Somer, W. Carrillo-Cabrera, E.M. Peters, K. Peters, H.G. von Schnering, Z. Kristallogr. 211 (1996) 635.
[245] R. Pöttgen, Z. Naturforsch. 50b (1995) 1181.
[246] R. Juza, F. Hund, Naturwiss 38 (1946) 121.
[247] R. Juza, F. Hund, Z. Anorg. Allg. Chem. 257 (1948) 1.
[248] J. Aubry, M. Fromont, R. Streiff, C. R. Acad. Sci. Paris C262 (1966) 1785.
[249] G. Cordier, A. Gudat, R. Kniep, A. Rabenau, Angew. Chem. Int. Ed. Engl. 28 (1989) 1702.
[250] J.M. McHale, A. Navrotsky, G.R. Kowach, V.E. Balbarin, F.J. DiSalvo, Chem. Mater. 9 (1997) 1538.
[251] A. Gudat, R. Kniep, J. Maier, J. Alloys Comp. 186 (1992) 339.
[252] M.Y. Chern, F.J. DiSalvo, J. Solid State Chem. 88 (1990) 459.
[253] J.F. Brice, J.P. Motte, J. Aubry, C. R. Acad. Sci. Paris C270 (1970) 1658.
[254] G. Cordier, A. Gudat, R. Kniep, A. Rabenau, Angew. Chem. Int. Ed. Engl. 28 (1989) 201.
[255] A. Gudat, Thesis, Universität Düsseldorf, Germany, 1990.
[256] A. Gudat, S. Haag, R. Kniep, A. Rabenau, J. Less-Common Met. 159 (1990) L29.
[257] J. Jäger, R. Kniep, Z. Naturforsch. 47b (1992) 1290.
[258] A. Gudat, R. Kniep, J. Alloys Comp. 179 (1992) 333.
[259] J.F. Brice, J. Aubry, C. R. Acad. Sci. Paris C271 (1970) 825.
[260] C.F. Baker, M.G. Barker, D.H. Gregory, in preparation.
[261] V. Schultz-Coulon, W. Schnick, Z. Naturforsch. 50b (1995) 619.
[262] D. Halot, M.J. Flahaut, C. R. Acad. Sci. Paris C272 (1971) 465.